



OPEN ACCESS

EDITED BY
Chao Yang,
South China University of Technology, China

REVIEWED BY
Hui Wang,
Southeast University, China
Yongbing Li,
Shanghai Jiao Tong University, China

*CORRESPONDENCE Zhanpeng Du, ⋈ dzp1014@163.com

RECEIVED 16 August 2025 ACCEPTED 14 October 2025 PUBLISHED 29 October 2025

CITATION

Du Z, Rui S, Ma B, Meng X, Ren L, Xu L, Yao F, Yu D and Cao C (2025) Research progress on riveting processes of low-ductility light alloys for carrier tools: a comprehensive review. Front. Mater. 12:1686963. doi: 10.3389/fmats.2025.1686963

COPYRIGHT

© 2025 Du, Rui, Ma, Meng, Ren, Xu, Yao, Yu and Cao. This is an open-access article distributed under the terms of the Creative Commons Attribution License (CC BY). The use, distribution or reproduction in other forums is permitted, provided the original author(s) and the copyright owner(s) are credited and that the original publication in this journal is cited, in accordance with accepted academic practice. No use, distribution or reproduction is permitted which does not comply with these terms.

Research progress on riveting processes of low-ductility light alloys for carrier tools: a comprehensive review

Zhanpeng Du^{1*}, Shili Rui², Baolin Ma^{1,2}, Xiangxin Meng^{1,2}, Lifang Ren^{1,2}, Liguo Xu², Feng Yao³, Dongzheng Yu³ and Can Cao³

¹Institute of Lightweight and Safety of New Energy Vehicle, School of Automotive and Traffic Engineering, Jiangsu University, Zhenjiang, China, ²Chery Automobile Co., Ltd., Wuhu, China, ³Suzhou Swangsea Intelligent Equipment Technology Co., Ltd., Suzhou, China

Energy shortage is a significant challenge faced by humanity, and energy conservation and carbon reduction are a common choice for global sustainable development. Among them, improving the lightweight level of carrier tools is a key way to promote global energy conservation and carbon reduction. Low-ductility light alloys have been gradually applied in the lightweight design of carrier tools due to their characteristics of high strength and low density. However, due to the large differences in physical properties such as melting points between low-ductility light alloys and high-strength steels, it is difficult to achieve effective connection of multi-material vehicle bodies, which limits the further promotion and application of low-ductility light alloy materials. As a cold joining technology, the riveting process has become an important means to support the mass application of low-ductility light alloy materials. In traditional riveting processes, solid rivets improve the uniformity of deformation by optimizing geometric and process parameters; blind rivets enhance the practicality of single-sided operation by regulating mandrel tension and deformation rate to suppress brittle fracture. New processes are constantly innovated: for example, self-piercing riveting without pre-opening reduces damage to the base material; pre-holed self-piercing riveting improves the bearing capacity of multi-layer dissimilar materials; adhesive-riveted hybrid joining has the advantages of strong bearing capacity and reliable connection; friction self-piercing riveting realizes the dual strengthening of "mechanical interlocking - solid-state joining" by softening materials through frictional heat; electromagnetic riveting improves the uniform deformation of materials through high strain rate dynamic loading. However, due to the low elongation and high sensitivity of low-ductility light alloy materials, the joints are prone to process-induced damage such as macroscopic cracks, which affect the forming quality and mechanical properties of the joints. Thus, it is necessary to deepen mechanism research, promote process optimization, expand the path of performance improvement in various environments, and promote the high-quality development of lightweight carrier tools.

KEYWORDS

carrier tools, low-ductility light alloys, riveting process, lightweight, connection performance, process optimization

1 Introduction

Carrier tools such as cars, aircraft, and rail transit vehicles are major sources of greenhouse gas emissions, and the task of energy conservation and emissions reduction has become increasingly urgent. In response, countries worldwide are enacting increasingly stringent emission regulations. For instance, the European Union's Euro 6 standard aims to limit the average CO₂ emissions from new passenger cars to no more than 60 g/km by 2030 (Järvikivi, 2021); the U.S. Environmental Protection Agency has established new standards for pollutants such as nitrogen oxides (NOx); and China has established a multi-dimensional policy framework to promote low-carbon industrial transformation, creating institutional synergies to achieve its "dual carbon" goals (Shen et al., 2025). Enhancing lightweighting levels is a key means of achieving energy conservation and emissions reduction in carrier tools, and the use of lightweight materials is an important pathway for promoting the lightweighting development of carrier tools (Anonymous, 2023; Weigi et al., 2023; Yılmaz et al., 2017). Figure 1 shows the recent trends in the development of multi-material body structures. As shown in the figure, the use of lightweight metal materials combined with high-strength steel has become the mainstream material selection approach for vehicle body lightweighting. Among these, die-cast aluminum alloys, magnesium alloys, and titanium alloys—three types of low-ductility lightweight metal materials—are most widely used in combination with highstrength steel. However, the significant differences in physical properties, such as melting points, between high-strength steel and low-ductility lightweight metal materials pose challenges for traditional spot welding processes in achieving effective bonding, thereby introducing new concerns regarding the service performance of carrier tools.

To overcome the inherent shortcomings of traditional spot welding processes in connecting high-strength steel and lowductility lightweight alloy materials, riveting offers an ideal alternative solution. As a mechanical joining method, riveting eliminates the need for high-temperature processes involved in welding, thereby fundamentally avoiding issues such as heat-affected zone embrittlement, grain coarsening, and the formation of brittle intermetallic compounds. This enhances joint toughness and is particularly suitable for material combinations with significant differences in thermal-physical properties, such as aluminum/steel and aluminum/titanium (Heidrich et al., 2021; Kim et al., 2019). In recent years, riveting technology for lightweight alloy connections has seen significant development: Solid rivet riveting forms rigid connections through traditional forging processes, offering strong static load-bearing capacity and addressing reliability issues in high-strength applications for lightweight connections (Grimm and Drossel, 2019; Mucha, 2014; Vorderbrüggen et al., 2022); Corepulling riveting enables single-side installation through its structural design, offering convenient operation and suitability for enclosed or narrow spaces, thereby improving connection efficiency in complex structures (Penalva et al., 2025; Tao et al., 2025; Tao et al., 2024); Self-piercing riveting (SPR) eliminates the need for pre-drilling holes, directly pressing into the sheet to form a lock, simplifying the process and enabling automation, thereby overcoming the efficiency bottleneck of traditional riveting requiring pre-drilling (Cacko, 2008; Danyo, 2014; Stephens, 2014; Zhao et al., 2022); Pre-holed self-piercing riveting guides deformation through precise pre-drilled holes, reducing resistance and enhancing adaptability to high-hardness, high-thickness materials, while lowering the risk of cracking associated with conventional self-piercing riveting (Liu et al., 2024; Wang et al., 2025c); Riv-bonding connection combine adhesive bonding with mechanical locking, enhancing overall performance through stress dispersion, offering excellent sealing and fatigue resistance, and addressing the performance shortcomings of single-mode connections (Gómez et al., 2007; Yang et al., 2025; Zhao et al., 2023); Friction self-piercing riveting (F-SPR) utilizes friction-generated heat to soften materials, simultaneously achieving stamping locking and interface bonding,

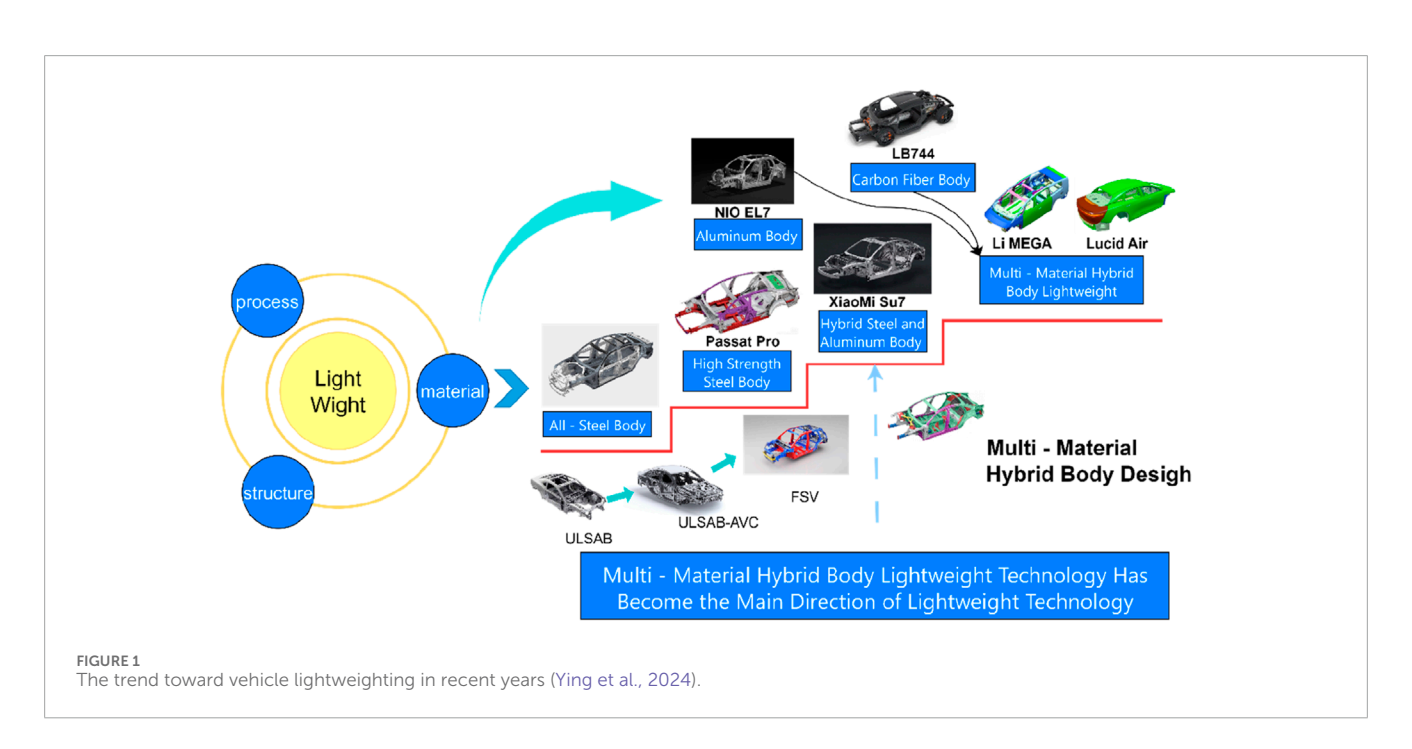


TABLE 1 Connection methods for light alloy materials.

| Riveting method | Advantage | Disadvantage | Application in transport vehicles | Picture |
|----------------------------------|---|---|---|---------|
| Solid rivet riveting | High strength and reliability Excellent sealing, vibration resistance | Requires operation on both sides, difficult to disassemble, heavy weight | Aircraft main beams, wing beams, bulkheads; ship keels, ribs, bulkheads | |
| Blind Rivet Riveting | Single-sided operation, convenient connection, high efficiency | Non-removable, limited load-bearing capacity | Instrument panel brackets, seat rails, luggage racks, window frames | 15 |
| Self-piercing riveting | Low energy consumption, easy to automate, environmentally friendly | Riveting equipment is cumbersome and complex, and cannot be used for single-sided riveting | Vehicle body, battery pack housing, thin steel plate and aluminum connection | |
| Pre-holed self-piercing riveting | Improve accuracy and consistency, Reduce restrictions on material performance | Increases process costs, sensitive to pre-drilled hole accuracy | Connection between the aircraft fuselage frame and skin | |
| Riv-bonding connection | High load-bearing and fatigue resistance, peel resistance and impact resistance | High manufacturing costs and lead times, and difficulties in maintenance | White body, doors, engine hood, battery pack housing, wing structure | |
| Friction self-piercing riveting | High-strength steel has good connection performance, reduces forming force | Generates heat-affected zones, equipment is complex and expensive | Body frame, chassis cross members and longitudinal members, battery pack shell frame | Ÿ |
| Electromagnetic riveting | No heat-affected zone, low static load, high repeatability | Expensive equipment, loud noise, and electromagnetic interference | Aerospace composite materials, heat-sensitive material components | |

making it suitable for connecting dissimilar materials and reducing brittle cracking during cold stamping (Ma et al., 2017; Xian et al., 2019). Electromagnetic riveting utilizes electromagnetic pulse force to drive rivets into high-speed forming, promoting plastic flow at high strain rates, resulting in superior forming quality and addressing the forming deficiencies of low-plasticity lightweight alloys (Cui et al., 2022; Jin et al., 2025; Jin et al., 2024). Table 1 below summarizes the connection methods for lightweight alloy materials. Different riveting technologies have distinct application scenarios and forming effects, so the appropriate method should be selected based on the properties of the connected components in practical applications.

Additionally, carrier tools are subjected to a wide range of complex vibration loads during actual operation, causing fasteners such as bolts and rivets to experience fatigue failure and loosening under severe impact and alternating loads (Li et al., 2021; Wang et al., 2024a), which significantly compromises the structural integrity and

safety of riveted joints (Ding et al., 2024; Wang et al., 2024e). To address this issue, numerical simulation technology demonstrates significant advantages. It enables the visualization and assessment of structural dynamic response processes (Liang et al., 2022; Tang et al., 2017; Xu et al., 2020; Zhu et al., 2022), optimization of riveting process parameters, prediction of joint performance, and evaluation of structural dynamic response. The specific techniques include: establishing a dynamic model (Robert et al., 2020) to effectively simulate the transient response and load transfer of rivets and connection interfaces in riveted structures under strong impact and alternating loads; modal analysis technology (Wang et al., 2024b) to reveal the natural vibration characteristics of riveted structures, identify resonance risk points, and lay the foundation for fatigue analysis; Discrete element method (Shi et al., 2017; Zhao et al., 2020) provides an in-depth analysis of rivet micro-contact, particle wear, and potential loosening mechanisms; extended finite element method (Chen et al., 2024a; Wang and Chen, 2020; Wang et al.,

2022) accurately predicts the initiation location of cracks around rivet holes, fatigue propagation paths, and final failure modes. These methods enhance the confidence in predicting riveting reliability and effectively identify areas prone to failure, providing theoretical basis and data support for optimizing riveting point layout and joint design. Furthermore, response surface methodology (RSM) (Chai et al., 2020; Guo Q. et al., 2019; Lu et al., 2016; Qi et al., 2025) is used to construct more efficient mathematical surrogate models, reducing optimization costs; while multi-objective genetic algorithms (Adade et al., 2024; Bonah et al., 2019) effectively explore complex design spaces to identify optimal process parameter combinations. These two optimization techniques significantly advance the efficient and reliable application of riveting in lightweight structures.

This paper aims to systematically review the research progress on low-ductility lightweight alloys for carrier tools and riveting processes. By analyzing the limitations of traditional riveting technologies and the innovative breakthroughs of new processes, it reveals the applicability patterns of different riveting methods in the connection of low-ductility lightweight alloys, providing theoretical references and technical pathways for addressing connection challenges in actual engineering applications. The paper is structured as follows: Chapter 2 discusses the current status and challenges of low-ductility lightweight alloys; Chapter 3 introduces the characteristics and applications of traditional riveting technologies; Chapter 4 focuses on the technical principles and research findings of new riveting processes; and Chapter 5 summarizes the current research progress and outlines future development directions.

2 Current status and challenges of low-ductility light alloys in carrier tools

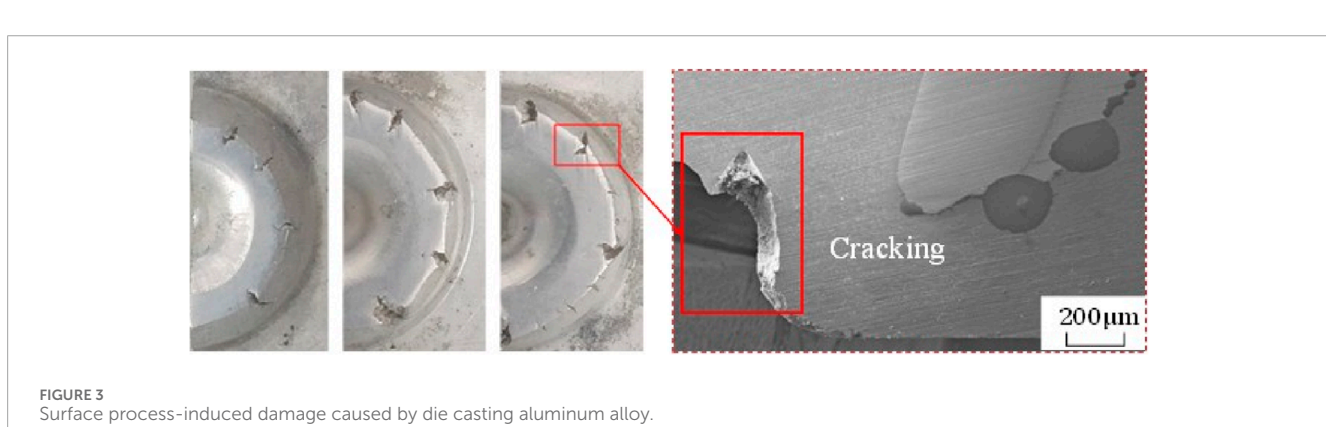
Currently, the main low-ductility light alloys used in carrier tools are die-cast aluminum alloys, magnesium alloys, and titanium alloys. Due to their different characteristics, the application in carrier tools also differ. The following is an analysis of the current status of these three low-ductility light alloys.

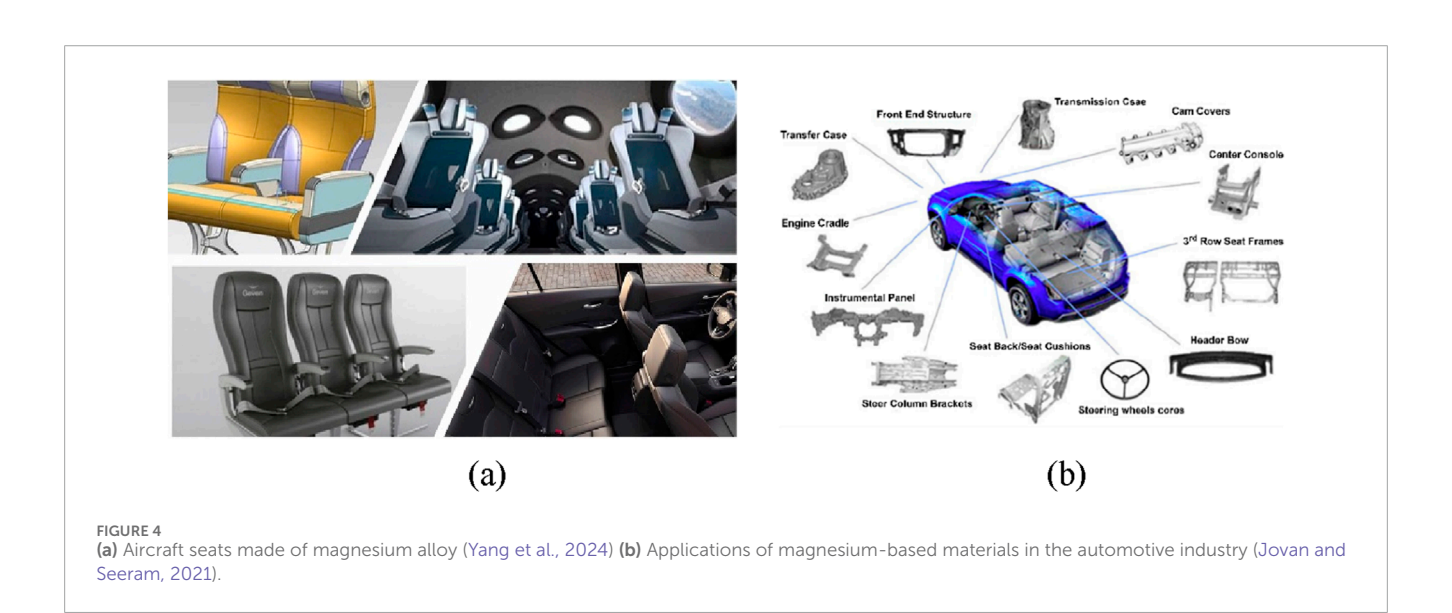
Die-cast aluminum alloys offer a moderate tensile strength, coupled with relatively low material costs, abundant raw materials, and high recyclability, making them widely used in industries such as automotive, aviation, and aerospace (Casarotto et al., 2012; Dong et al., 2025). For example, in 2021, the Tesla Model Y became the first vehicle to adopt large-scale one-piece die-cast aluminum alloy, significantly enhancing the vehicle's lightweight design. Subsequently, Chinese automotive companies such as NIO, Xpeng, and Xiaomi began to develop die-casting technology and successively launched steel/die-cast aluminum alloy hybrid body products, driving the rapid development of die-cast aluminum alloy in vehicle bodies, as shown in Figure 2. In the aerospace field, die-cast aluminum alloys are primarily used in the structural components of spacecraft rocket fuel tanks, spacecraft fuselages, and large pressurized cabins of manned spacecraft (Li et al., 2023). However, die-cast aluminum alloys are prone to porosity defects and thermal cracking tendencies during production (Réger et al., 2023). For example, Cao et al. (2024) found that casting process parameters significantly influence the evolution of porosity defects, reducing material mechanical properties and sealing performance. Additionally, traditional die-cast aluminum alloys requiring heat treatment exhibit high welding defect rates due to internal gas pores, while non-heat-treated types show some improvement but still lag behind other materials in welding characteristics. In practical applications, vibrational environments can easily lead to connection issues (Pang et al., 2019), and such defects may exacerbate stress concentration and the risk of fatigue crack initiation (Chen et al., 2020). Furthermore, die-cast aluminum alloys have relatively low elongation, and during riveting processes, their surfaces are prone to developing "serrated" macro-cracks (as shown in Figure 3), which can impair the service characteristics of transport vehicles.

Magnesium alloys are the lightest engineering metals, offering significant weight reduction benefits and excellent damping properties (Qin et al., 2015), making them highly attractive in industries such as aerospace and automotive (Chen et al., 2024b; Liu B. et al., 2023; Wang et al., 2024f). Figure 4 below illustrates some applications of magnesium alloys. Additionally, magnesium alloys, due to their low melting point and excellent fluidity, can be processed using die-casting techniques to extend mold lifespan and reduce production costs. Breakthroughs in super die-casting technologies like Tesla's Giga-Casting have further driven their widespread adoption in large automotive structural components (Tian et al., 2023). In the automotive sector, magnesium alloys are primarily used in components such as seat frames and instrument panel brackets. Research by the Bo team (Zhan et al., 2025) indicates that magnesium alloys reduce the weight of these automotive components by 25%-30%. In the aerospace sector, magnesium alloys are used in critical components of aircraft, spacecraft, and satellites (Yang et al., 2024). The G04 magnesium alloy has been successfully applied to the electrical cabinets of the manned spacecraft, reducing weight by approximately 13 kg (Bai et al., 2023); In the rail transit sector, magnesium alloys are primarily used in structural components such as luggage racks inside highspeed trains, enhancing their lightweight design and facilitating installation and maintenance (Zhang J. et al., 2023). Although magnesium alloys have achieved some level of application across various fields, their high cost remains a significant barrier to large-scale adoption; their low elongation rate also leads to severe process-induced damage during connection processes, necessitating the exploration of more effective application methods.

Titanium alloys, as lightweight high-strength materials, have a density ranging from 4.5 to 4.6 g/cm³, combining ultra-high tensile strength with excellent corrosion resistance, significantly reducing maintenance requirements, and are widely used in carrier tools. In the aerospace industry, it is used to manufacture aircraft engine blades, turbine disks (Peters et al., 2003; Singh et al., 2017), and other components. Titanium alloy landing gear components can reduce weight by approximately 15%-35% compared to steel components while withstanding significant impact (Singh et al., 2017); In the space industry, satellite mounts utilize its high strength and resistance to space environment corrosion to ensure long-term stable operation (Borba et al., 2018); in the marine industry, high-performance propellers are made of titanium alloy, effectively resisting seawater corrosion and improving propulsion efficiency (Ma et al., 2025). As shown in Figure 5, some applications of titanium alloy. However, the practical application of titanium

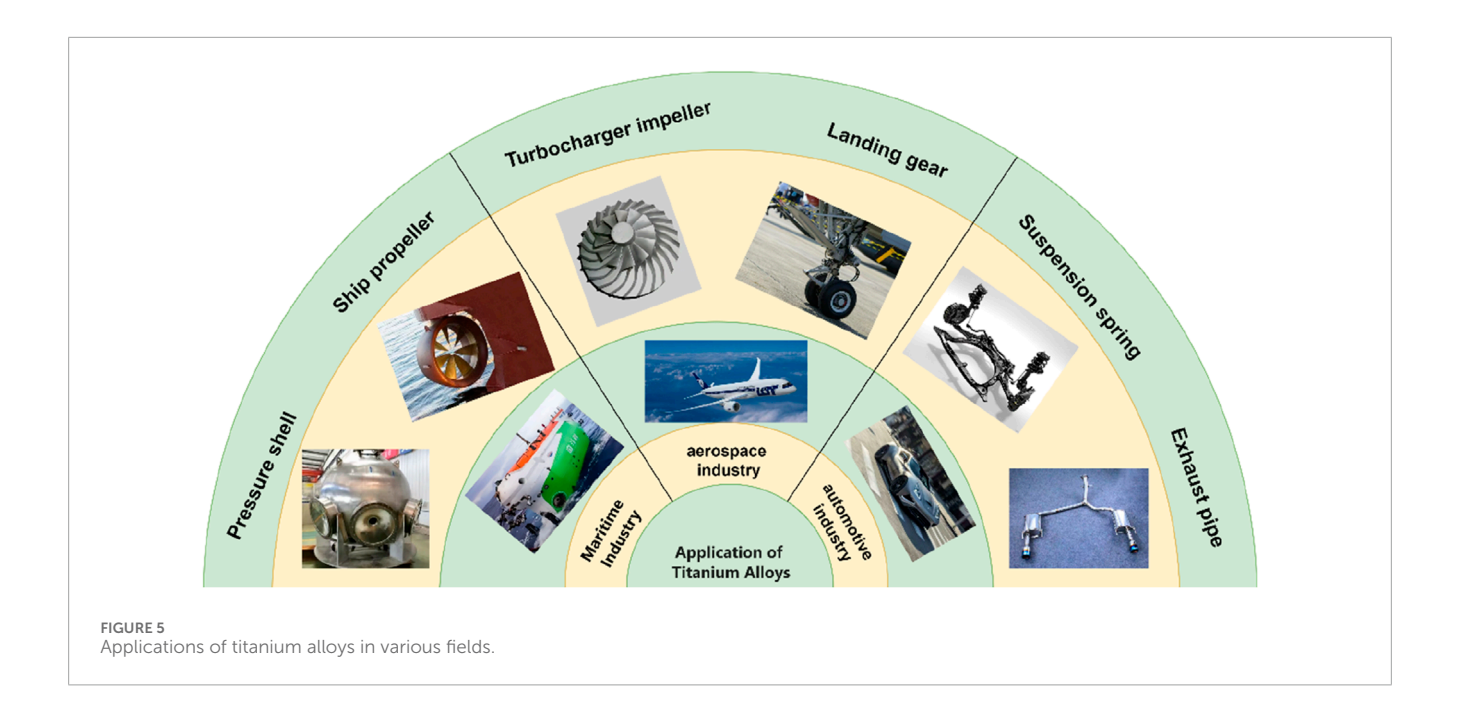






alloys also faces the following challenges: Difficulty in connecting dissimilar materials. Chen et al. studied laser welding of titanium alloys with nickel-based Inconel 718 alloys, requiring precise control of heat input and laser deflection to suppress brittle phases and defects (Chen et al., 2011). Extremely high cost, which

can be more than 10 times that of aluminum alloys, greatly limiting its large-scale application (Liu et al., 2020). Processing difficulties, requiring specialized equipment and complex processes. For example, manufacturing high-strength thin-walled titanium tubes necessitates special techniques such as the step-cooling



spinning method developed by Xie et al. (2026). Recent research is addressing these challenges through surface modification (e.g., the dual-layer ${\rm TiO_2/PDMS}$ superhydrophobic coating developed by Ma et al., which significantly enhances corrosion resistance to 99.88%) (Ma et al., 2025) and deep cryogenic treatment (e.g., Liu et al. demonstrated that it can refine grain size, increase dislocation density, and reduce stress corrosion sensitivity) (Liu et al., 2025). However, cost control and process simplification remain the primary factors limiting its broader application.

The aforementioned three types of low-ductility lightweight alloys, with their excellent lightweight potential and specific properties, are increasingly being used in critical components of carrier tools. However, the inherent challenges in manufacturing, usage, or cost significantly increase the difficulty of assembling and connecting structural components and applying them on a large scale. Traditional connection processes such as spot welding often yield poor results or are cost-prohibitive when applied to these materials. Therefore, exploring and developing efficient and reliable connection technologies suitable for low-ductility lightweight alloy materials, particularly the innovation and optimization of riveting processes, has become a critical step and one of the most pressing issues to address in driving their broader application.

3 Normal riveting technology

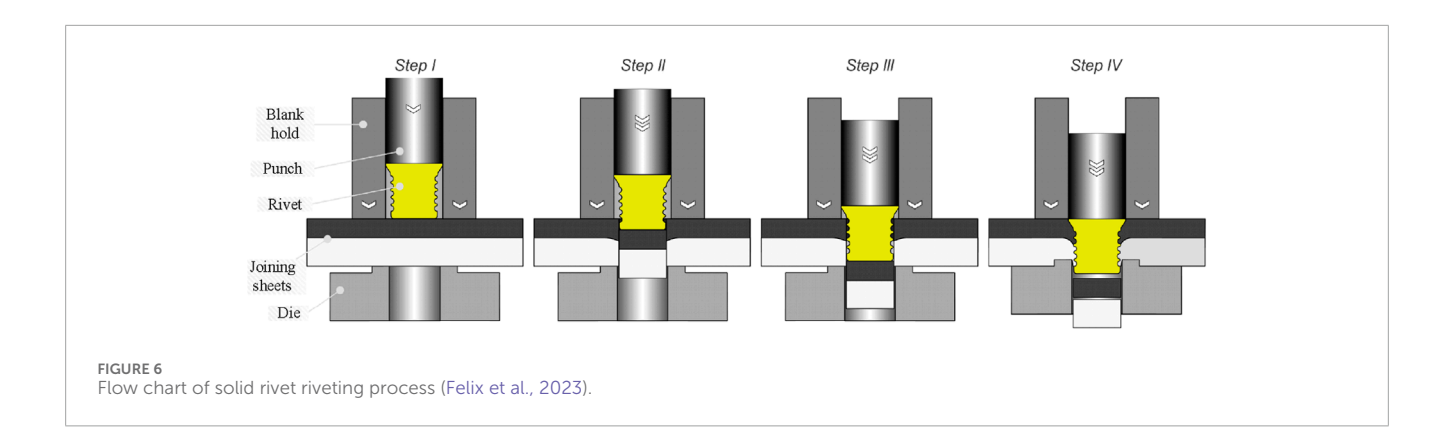
3.1 Solid rivet riveting

Solid rivet riveting is a classic joining process. The process is as follows: first, the sheets are fixed between the blank holder and the die of the installation tool (Step I); then, the punch drives the rivet through the connecting plates (Steps II and III); the material of the lower sheet is pressed into the circumferential groove of the rivet (Step IV), thereby fastening the connected parts together, as shown in Figure 6 (for solid self-piercing riveting) (Felix et al., 2023). This

process is widely used in fields such as aerospace and automotive manufacturing. Its core lies in controlling the uniformity of rivet deformation to avoid cracking of low-ductility materials.

Solid rivets play the dual role of punching tools and fasteners during the joining process, which puts extremely high requirements on the strength and ductility of the rivets. Optimizing process parameters is a key means to improve product performance, and methods of experimental verification, numerical simulation and algorithm optimization are often used. In algorithm optimization, spectral analysis techniques such as near-infrared, Raman and hyperspectral, combined with chemometric algorithms such as partial least squares, synergetic interval partial least squares, genetic algorithm-partial least squares, and ant colony optimization-partial least squares, have realized rapid qualitative and quantitative analysis of food components, quality and pollutants. Their ideas of variable selection and model optimization provide a reference for the experimental verification of material joining process parameters (Arslan et al., 2019; Arslan et al., 2018; Bonah et al., 2019; Guo Z. M. et al., 2019; Hu et al., 2017; Khulal et al., 2016; Kutsanedzie et al., 2018; Li et al., 2019; Qin et al., 2019; Sun et al., 2018; Sun et al., 2017; Tang et al., 2021; Zhou et al., 2020; Zhou et al., 2019). Numerical simulation methods such as computational fluid dynamics, discrete element method and CFD-DEM coupling have shown high precision in simulating equipment flow field characteristics, material separation and transportation processes, and their simulation methods for multi-physics field coupling and dynamic processes can provide reference for the numerical simulation of riveting processes (El-Emam et al., 2023; Fordjour et al., 2020; Jiang et al., 2017; Liu J. P. et al., 2023; Shi et al., 2019; Tang et al., 2017; Xu et al., 2016; L. Z. Xu et al., 2020; Yuan et al., 2023; Zhu et al., 2022).

To achieve reliable connection, regarding the collaborative optimization of material selection and geometric design, Grimm and Drossel (2019) aimed at the problems of insufficient locking and rivet fracture when traditional rivets connect high-strength



materials, and clarified the influence laws of geometric parameters such as rivet shank taper and head thickness, through numerical simulation and experimental validation methods, the influence of parameters such as the rivet shank taper and head height on the interlock value was clarified. Ping et al. (2025) focused on the optimization of process parameters for dissimilar material joining, and adopted the solid rivet resistance riveting welding process to join aluminum/steel dissimilar materials, thereby successfully avoiding the formation of brittle intermetallic compounds. To further improve the performance of solid rivet joints, Xu and Wang (2021) proposed an integrated multi-objective optimization framework of "material-structure-process-performance," and optimized the solid rivet connection of magnesium/aluminum composite structures combined with methods such as Taguchi, which verified the effectiveness of this method in the optimization of connection parameters for low-ductility light alloys.

Factors such as different material and thickness combinations have a significant impact on the connection performance of joints. Jacek (2013) systematically studied the connection ability of solid rivets to low-ductility materials through single-lap shear tests and single-edge tearing tests. The results showed that the type of sheet material is the most critical factor affecting joint strength, and the greater the thickness, the more significant the influence of material type. Samuel and Olaf (2010) deeply analyzed the installation process of solid rivets in T351 aluminum alloy components and the influence of the clearance fit between rivets and holes, clamping length and extrusion strength on residual stress and contact force through FEM simulation modeling. The high agreement between the simulation results and experiments, including the forming geometry of the rivet head and the force-displacement curve, verified that the model can effectively predict the mechanical properties of joints, providing a quantitative tool for the optimization of riveting process parameters for low-ductility aluminum alloys used in aerospace.

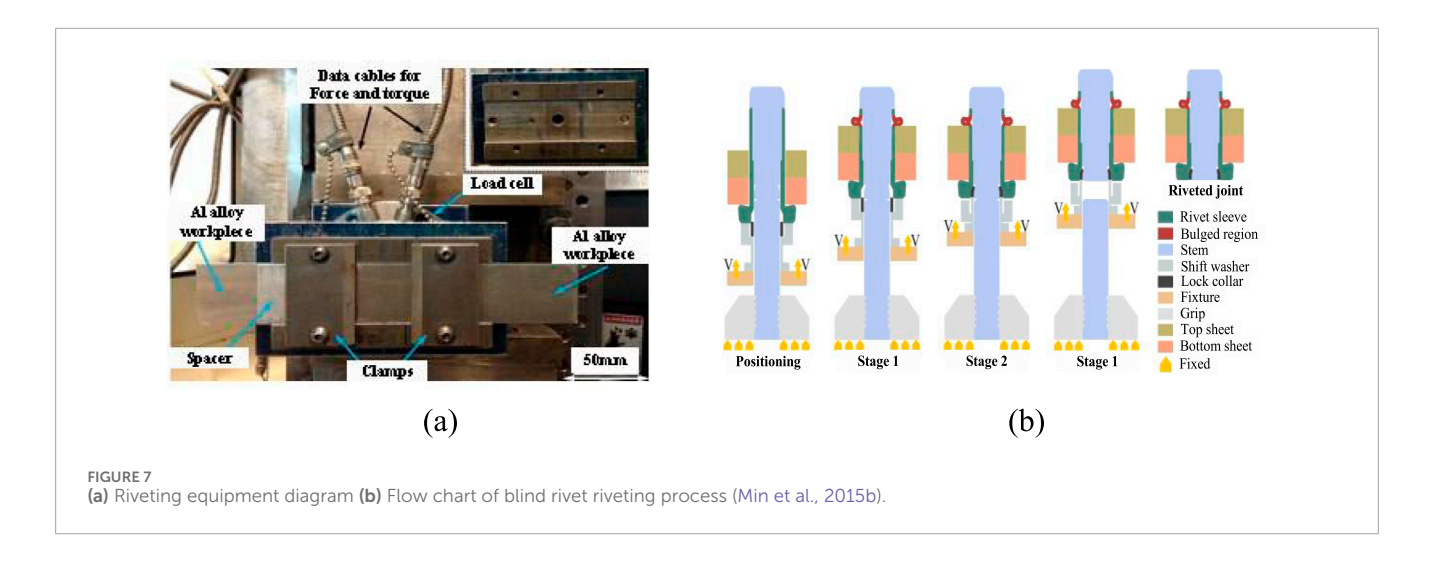
For the solid rivet connection of large carrier tool structures such as antenna reflectors and vehicle body frames, deformation caused by positioning deviation is a core problem. Ni et al. (2017) measured the coordinates of key points of positioning deviation, simulated the deformation under different rivet upsetting directions and assembly sequences, and optimized the process parameters through virtual plane calculation, which significantly reduced the riveting dimensional error of large aluminum components and solved the

problem of assembly accuracy caused by poor plastic deformation ability of low-ductility materials. In addition, Wang et al. (2019) determined the constitutive parameters for predicting the dynamic behavior and failure of riveted joints through material testing and modeling, providing a theoretical basis for the performance prediction of solid rivet connections under impact loads of carrier tools.

3.2 Forming process simulation and validation

Blind rivet riveting (also known as blind riveting) utilizes the special structure of blind rivets and is suitable for single-sided operation scenarios. The riveting process includes three consecutive stages: bulge formation, lock ring engagement and valve stem fracture, so as to realize the connection of workpieces, as shown in Figure 7b (Min et al., 2015b). This process is operationally convenient; however, when used with low-ductility materials, careful control of the expansion force is essential to prevent material brittle fracture.

Regarding the fatigue damage problem during the joining process, Li et al. (2016) pointed out that the damage of CFRP during installation is mainly matrix extrusion crushing, while the aluminum alloy side is prone to plastic deformation of the hole wall. Interference fit can significantly improve the bearing strength of CFRP/Al single-lap blind riveted joints during the installation stage. Zhao et al. (2021) found through finite element analysis that the shear bearing capacity of stainless steel blind riveted connections increases linearly with the number of rivets, and plastic bending is prone to occur due to the low elastic limit of the material. It is suggested that the group rivet effect coefficient can be ignored in design, providing a reference for the structural design of blind riveting for low-ductility light alloys. The SPH-FEM coupling model of Wang et al. (2018) revealed the energy conversion law in Mg/Al blind riveting. The frictional heat generated by torque accounts for the dominant part of the total energy consumption, the maximum temperature on the Mg side is slightly higher than that on the Al side, and the interface interlocking formed by material flow is the key guarantee for joint strength. In the Al-Mg blind riveted joints on the hull, the Mg side undergoes uniform corrosion due to the alkaline crevice environment, while the Al side experiences crevice and galvanic corrosion, which puts forward special requirements



for the protection of magnesium alloy-aluminum alloy joints in shipborne carrier tools (Li et al., 2018).

Process parameters are important factors affecting connection quality, so optimizing process parameters is an important way to achieve efficient connection. Wang G. et al. (2024) found through finite element simulation that when the hole diameter increases, the protruding dimensions of the mandrel and lock ring increase, and the contact stress between the sleeve and the mandrel as well as the connecting plate increases; when the interlayer thickness increases, the contact stress first increases and then stabilizes, while the contact stress between the lock ring and the sleeve first increases and then decreases. In addition, the influence of sleeve geometric parameters cannot be ignored. Feng et al. (2024) studied that two key geometric parameters of the sleeve will change the shape of the blind end and the distribution of the bearing area, thereby affecting the damage degree of CFRP. Reasonable design can reduce material crushing and improve joint integrity. Aiming at the problem of simulation accuracy caused by the gradient hardness distribution of blind rivets, Tao et al. (2024) proposed a hardness-based Johnson-Cook constitutive model. By introducing a hardness compensation term, the stress prediction error was significantly reduced, which can accurately simulate the bulge forming process of A286 superalloy blind rivets. Their subsequent research also found that the strain gradient in the bulge area after riveting will drive grain refinement and increase in dislocation density, among which the contribution of dislocation strengthening to yield strength reaches 53.3%–57.3%, providing a theoretical basis for the performance control of lowductility light alloys after riveting (Tao et al., 2025). Bothiraj et al. (2023) used Taguchi method and ANOVA analysis and found that the strength of friction stir blind riveted joints is comprehensively affected by rivet material, diameter, sheet combination and spindle speed. Among them, rivet material has the greatest influence; within a certain range, the strength increases with the increase of spindle speed, but when the speed is too high, the strength decreases due to overheating.

The process innovation of blind rivets is constantly developing, and the connection performance has made significant breakthroughs through continuous optimization and innovation of blind riveting processes. The new single-step blind riveting method developed by Min et al. (2015a) makes the maximum tensile load

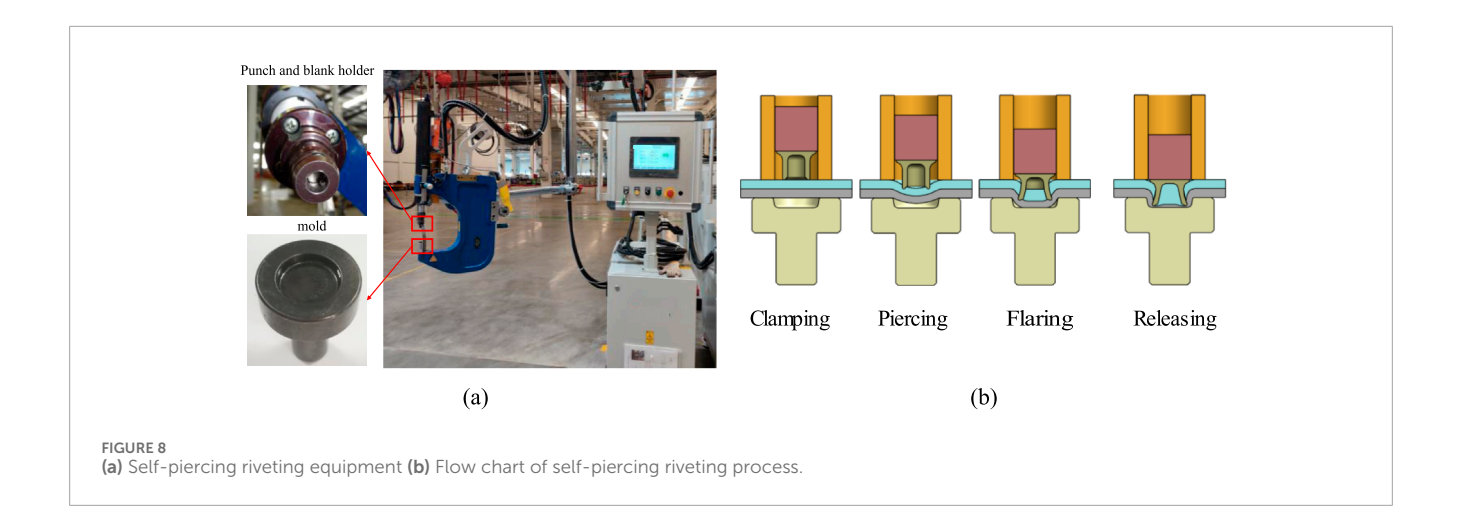
of the joint 20% higher than that of traditional blind riveting and 11% higher than that of friction stir blind riveting, which is suitable for dissimilar connections between magnesium alloys and aluminum alloys. Subsequent research on AA6111/AA6022 joints showed that the maximum tensile load of friction stir blind riveting increases slightly with the increase of feed rate, and the joint failure presents a "shear-tearing" composite mode. Microhardness tests show that the stir zone has a hardness peak due to strain hardening (Min et al., 2014). The pre-holed friction stir blind riveting (FSBR-pH) process developed by Ali et al. (2022) solves the applicability problem of traditional processes in pre-drilled components by optimizing stirring parameters, and is suitable for the connection of magnesium and aluminum alloys in hardto-reach areas such as aircraft cabins. Lu et al. (2023) provided a performance prediction tool for the hybrid connection of lowductility light alloys and composites through numerical simulation methods. In terms of quality monitoring, the two methods proposed by Penalva et al. (2025), manufacturing chain analysis and deep learning image recognition, have a prediction accuracy of over 0.9 for the installation quality of blind rivets, providing technical means for defect detection in automated production. In special working condition applications, the flow drilling riveting process proposed by Zhang K. et al. (2022) predicts penetration force and torque through a thermal-mechanical coupling model, with a temperature prediction error ≤4%, providing ideas for parameter optimization of titanium alloy blind riveting in high-temperature environments.

4 Novel riveting technology

4.1 Self-piercing riveting process

4.1.1 Process principle and flow

Self-piercing riveting (SPR) is an efficient cold joining technology, which is suitable for connecting dissimilar materials. As shown in Figure 8b, it is divided into four different steps: (1) Clamping, where two sheets are pressed against the die by a blank holder; (2) Piercing, where the upper sheet is split into two parts by a semi-tubular rivet driven by the punch; (3) Flaring, where the



rivet tail starts to spread into the lower sheet, causing interlocking deformation between the two sheets; (4) Release, where the punch retracts and releases (Du et al., 2021a).

4.1.2 Key influencing factors and process optimization

The die structure is a primary factor influencing the formation quality, and its structural parameters directly affect material flow, interlock formation and cracking risk of low-ductility materials. Process parameters directly affect the homogeneity of the joint's microstructure by governing material flow behavior, which in turn determines its mechanical properties.

In addition to die and process parameters, the material selection and surface coating of rivets are also key factors affecting the quality of SPR joints, as both directly determine the joint's load-bearing capacity, corrosion resistance, and compatibility with dissimilar base materials. For the joining of low-ductility light alloys, rivet materials must balance strength matching and galvanic corrosion avoidance: for aluminum-based multi-material joints, aluminum alloy rivets (such as AA5052-O and AA6061-T6) with thermal expansion coefficients similar to those of the base materials are often used. As noted by Zhang H. et al. (2024) in their study on the adaptation of spherical dies to low-ductility materials, AA6061-T6 can reach a tensile strength of 310-340 MPa after solution and aging treatment, ensuring load-bearing capacity while maintaining a certain degree of ductility, which can effectively avoid brittle fracture during the piercing process. When joining high-hardness materials, Wang et al. (2024c) pointed out in their analysis of the rivet hardness matching requirements for different stacking combinations that high-strength steel rivets (such as boron steel B1500HS and martensitic stainless steel 17-4 PH) can achieve a yield strength exceeding 1,200 MPa after quenching and tempering treatment, preventing rivet shank deformation during piercing. For CFRP/aluminum hybrid joints, Zhang et al. (2020) found in their research on pre-holed self-piercing riveting that titanium alloy rivets have a small galvanic potential difference with CFRP, which can avoid interface corrosion, and their high specific strength helps reduce the additional weight of the structure.

Surface coatings further improve the durability and process adaptability of rivets: SPR joints in automotive chassis or marine carrier tools are prone to contact with corrosive media. As

mentioned by Wang et al. (2024a) in their optimization of aluminum alloy blind riveting process parameters, steel rivets with an $8-12 \mu m$ thick zinc-nickel alloy coating have 5-10 times the corrosion resistance of traditional zinc-plated coatings and can achieve no red rust for more than 1,000 h in neutral salt spray tests. For the SPR joining of high-hardness materials such as AA7075-T6, Lun et al. (2025) found in their comparison of the effects of different dies on AA5052 joints that an Al₂O₃-TiO₂ ceramic-based coating can reduce the friction coefficient between the rivet and the base material from 0.35 to 0.18, decrease the piercing force by 15%-20%, and avoid scratches on the base material surface. In adhesive-riveted hybrid joints, Liu et al. (2024) pointed out in their study on the effect of pre-holing on self-piercing adhesive-riveted joints that phosphate conversion coatings enhance mechanical interlocking with adhesives through their porous structure, which can increase the interfacial shear strength by 20%-30% and optimize the overall performance of the joint.

Huang et al. (2024) studied dissimilar joints and found that the die type and size significantly affect the material distribution and forming quality of the lower sheet; increasing the rivet height will significantly improve the interlock amount and effective thickness; the filling state of the die groove directly determines the expansion degree of the rivet. Lun et al. (2025) compared the effects of flat, convex and spherical dies on AA5052 joints. The flat die can obtain the maximum interlock value and optimal mechanical properties, but the rivet head height is higher, resulting in slightly inferior forming quality to the convex die; the spherical die has poor forming quality and mechanical properties due to limited material flow. However, Zhang Z. et al. (2024) pointed out that a spherical die is more suitable for low-ductility materials. When parameters are appropriately set, it can avoid sheet cracking and form a highstrength interlock. The key lies in the fact that a moderate strain rate prevents the initiation of micro-cracks caused by uneven plastic flow in low-ductility materials.

The matching between the die and the rivet is also crucial to the forming quality of the joint. Silvayeh et al. (2024) found that although the offset between the rivet and the die will change the symmetry of the joint, as long as the interlock amount is sufficient, the impact on shear strength is limited. The reshaped self-piercing riveting proposed by Wu et al. (2025) realizes secondary flaring by

optimizing the die structure, which improves the shear strength and solves the bottom defect problem of traditional SPR. In addition, Wang et al. (2024a) pointed out that different stacking combinations need to be matched with rivets and dies of specific hardness. Wang C. et al. (2023) proposed that T6/T7 heat treatment reduces cracks by reducing the yield strength for the connection of die-cast aluminum alloys and high-strength steels, significantly improving the energy absorption of joints. Ying et al. (2021) confirmed that thermal self-piercing riveting can significantly improve connectivity after increasing the riveting temperature, and the load angle and speed have a significant impact on mechanical properties.

4.1.3 Joint performance characterization

The quality of die design ultimately needs to be verified by joint performance. In terms of static mechanical properties, the multiple nonlinear regression model established by Chen et al. (2022) for various aluminum alloys shows that the joint failure load and maximum riveting force are mainly affected by the interaction between sheet thickness and rivet hardness, and the model prediction error is small, providing a quantitative basis for parameter optimization. The friction self-piercing riveting developed by Li et al. (2024) achieves crack-free connection through die design control; the D2 die, due to the synergistic effect of mechanical interlocking and solid-state bonding, has a single-lap shear strength of 11.57 kN. Duan et al. (2023) found that the smaller the edge riveting distance, the lower the maximum shear load and energy absorption, and the joint strength based on the upper sheet is better.

In terms of dynamic and corrosion performance, Du et al. (2021b) compared and found that aluminum-steel SPR joints exhibit a higher peak force under dynamic loading compared to quasi-static loading, yet with lower energy absorption. This indicates a reduction in the material's plastic deformation capacity at high loading rates, where the accumulation of microscopic damage more readily leads to brittle failure. Chen et al. (2025) found in AZ31/PEEK dissimilar joints that the early corrosion current density of SPR joints is higher than that of friction stir spot welded joints, but the residual strength after immersion is twice that of the latter, and the longterm stability of the mechanical interlock structure is better. The equivalent simplified model established by Duan et al. (2023) can accurately simulate the collision response of steel-aluminum hybrid beams, and found that increasing the load angle is prone to cause beam instability, and at this time, rivet failure has a significant impact on energy absorption. Zhang et al. (2025a) studied the influence of axial compression on 5083 aluminum alloy joints, showing that 60-80 kN compression can improve section parameters but increase the risk of rivet cracks.

4.1.4 Existing problems and future directions

SPR, through the optimization of die parameters and regulation of joint performance, exhibits excellent adaptability to dissimilar materials and stability under complex working conditions—these merits have made it a crucial technical means in the manufacturing of lightweight transportation vehicles. In current mechanism research, although numerical simulation can analyze forming stress, strain, and impact response, it lacks investigation into the influence of microscopic damage. Future efforts should focus on three key directions: first, advancing the intelligent design of dies and rivets;

second, conducting morphology research under the multi-field coupling mechanism; and third, establishing a multi-scale numerical simulation platform to provide support for the technical application under various working conditions.

4.2 Pre-holed self-piercing riveting

4.2.1 Process principle and flow

Pre-holed self-piercing riveting (PH-SPR) builds on the conventional SPR process by incorporating a pre-hole step. By optimizing the hole diameter to guide material flow, it enhances the quality of the interlock structure. A hole with a specific diameter is pre-processed on the sheet to be connected, and then a self-piercing rivet is used to rivet the sheet through the pre-holed hole. A mechanical interlock structure is formed through the plastic deformation of the rivet and the sheet, thereby realizing the connection of dissimilar or similar materials. The specific process is shown in Figure 9.

4.2.2 Key influencing factors and process optimization

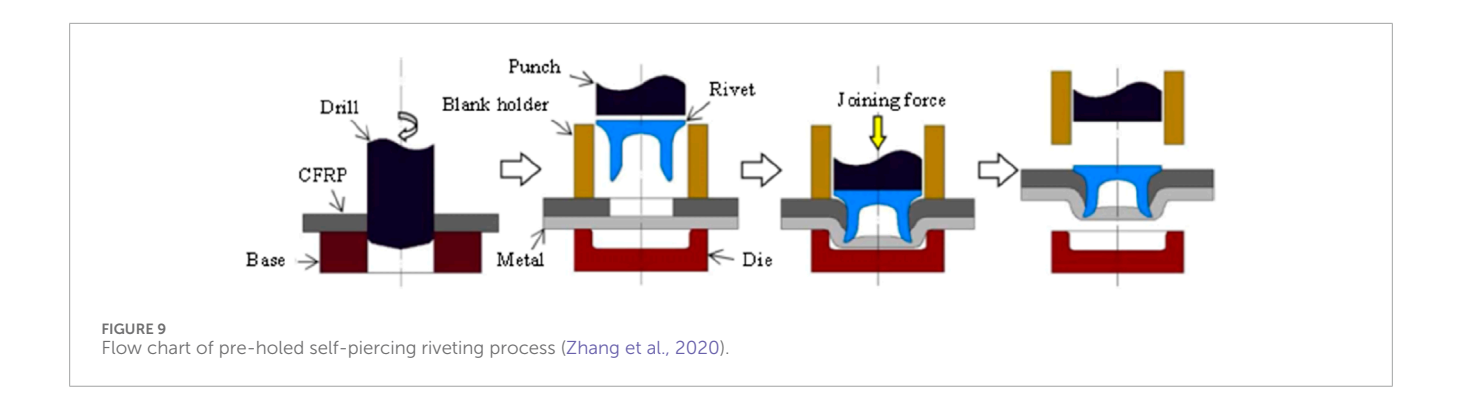
This process is particularly suitable for joining multi-layer dissimilar materials. Wang et al. (2024b) studied the influence of process parameters on the performance of PH-SPR joints and showed that increasing the sheet thickness improves the peak load; when the hole diameter increases, the peak load of 1.6 mm steel sheets decreases faster than that of 1.2 mm steel sheets. This indicates that an excessively large aperture may lead to an insufficient interlock structure, creating stress concentration points at the interface which can become initiation sites for fatigue cracks.

Under dynamic loading conditions, the strain rate effect makes the shear peak load increase linearly with the loading speed; the combination of 1.2 mm steel sheets and 5.5 mm hole diameter is more significantly affected by the loading speed, and the peak loads of shear, peel and cross-tension joints all increase with the speed, among which the cross-tension joints have a larger increase (Wang et al., 2025a).

4.2.3 Joint performance characterization

To evaluate its joining effectiveness, researchers have conducted in-depth analyses of the mechanical properties and durability of PH-SPR joints. Zhang et al. (2020) found in the connection research of carbon fiber reinforced polymer laminates and pure titanium sheets that PH-SPR can reduce the strength loss of rivets and enhance the hardening effect of titanium sheets; when the failure mode is rivet pull-out, the strength is significantly higher than that of CFRP layer tearing, and the interlock length is the key factor determining joint strength.

Under extreme working conditions coupling corrosive environments and dynamic loads, the performance of PH-SPR joints degrades significantly. For example, in a neutral salt spray test simulating the marine atmospheric environment (e.g., 5% NaCl solution, sprayed at 35 °C), steel-aluminum dissimilar material joints undergo severe galvanic corrosion due to the galvanic effect, and the aluminum plate is rapidly corroded as the anode (Wang et al., 2025b). Corrosion products accumulate at the riveting interface to generate expansion stress, and the corrosion pit itself, as a stress



concentration point, greatly accelerates the initiation of fatigue cracks. Wang et al. (2025c) conducted experiments in a salt spray corrosion environment and showed that the peak force of PH-SPR joints without adhesive bonding decreased by 27.4% after 720 h of corrosion, while the combination of electrophoretic coating and adhesive bonding can basically offset the corrosion impact; even if corroded, the peak force of PH-SPR-adhesive joints is still much higher than that of uncorroded PH-SPR. In terms of fatigue performance, increasing the hole diameter will shorten the fatigue life, while increasing the sheet thickness can extend the life. Studies have shown that the fatigue life of J16-5.5 joints with 1.6 mm steel sheets and 5.5 mm hole diameter under 5.0 kN load is 5.3 times, 7.8 times and 3.98 times that of J12-5.5, J12-6.0 and J16-6.0 respectively. Stress concentration and fretting wear are the main causes of fatigue fracture (Wang et al., 2025a).

4.2.4 Existing problems and future directions

In summary, PH-SPR adopts a joining mode that first uses predrilled holes for guidance followed by self-piercing riveting. This mode can effectively improve the interlocking uniformity and loadbearing capacity of joints for high-hardness, high-thickness, and multi-layer dissimilar materials. In current mechanism research, however, there is still a lack of investigation into two key aspects: first, the relationship among pre-hole size, strain rate, and strength under dynamic loads; second, the law of corrosion-fatigue coupled damage. For future work, efforts should focus on four directions: establishing a global process optimization model based on intelligent algorithms; conducting *in situ* research on dynamic-corrosion coupled damage; developing an integrated simulation tool for "process-performance-lifespan;" and promoting large-scale application by combining low-cost surface treatment technologies.

4.3 Adhesive-riveted hybrid joining process

4.3.1 Process principle and flow

The adhesive-rivet hybrid joining process is an innovative riveting technology that combines adhesive bonding with mechanical riveting to fully leverage the advantages of both joining methods. As shown in Figure 10a, the process is as follows: (1) Surface treatment: remove oil stains on the base material, polish and clean debris on the material surface; (2) Applying adhesive layer: evenly apply the adhesive on the lower surface of the sheet; (3) Performing SPR connection: at this stage, the upper sheet and the

adhesive layer are split into two parts by the semi-tubular rivet driven by the punch, and the rivet tail finally spreads into the lower sheet, causing interlocking deformation between the two sheets; (4) Curing: put all Riv-Bonding joints into an oven to cure the adhesive layer; (5) Cutting joints: all joints are cut along the center line of the rivet points; (6) Finally, quality evaluation is carried out (Du et al., 2025).

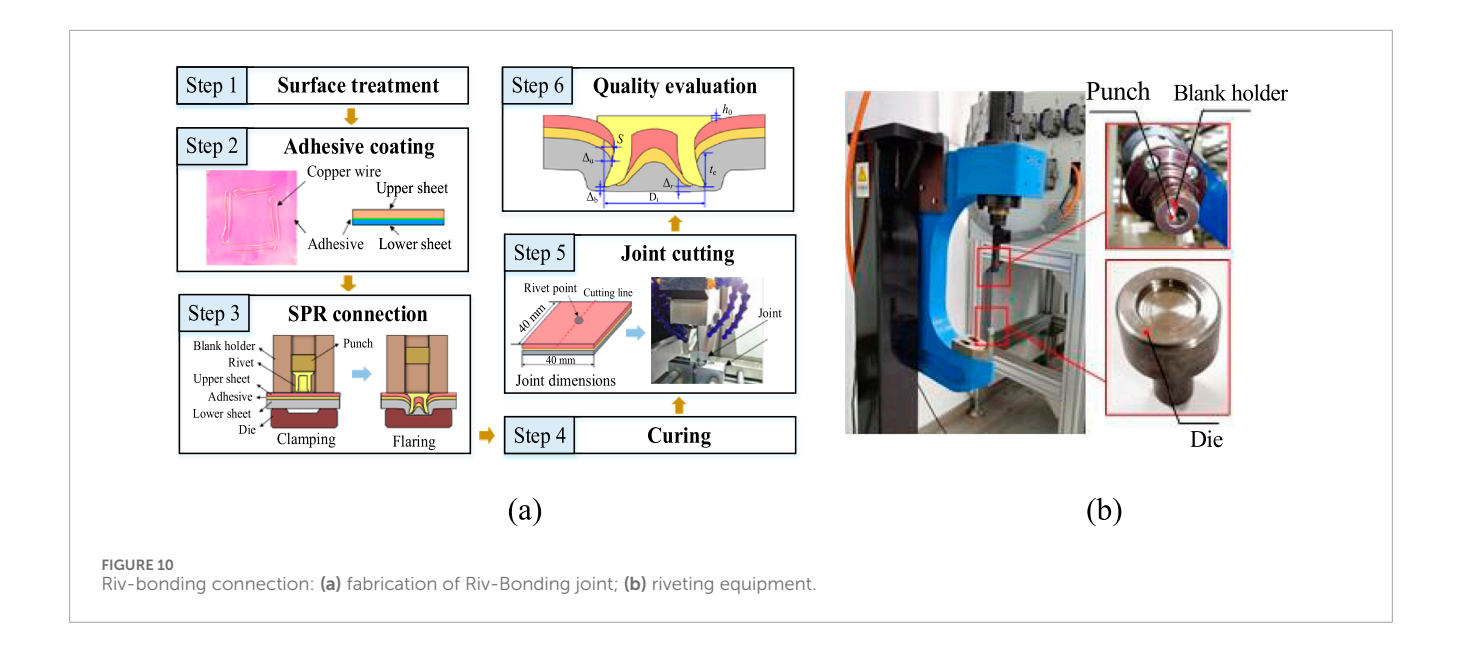
4.3.2 Key influencing factors and process optimization

Rivet riveting is prone to local stress concentration, and adhesive bonding will have reduced connection performance in high-temperature or impact environments. The adhesive-riveted hybrid joining process combines adhesives with riveting technology, giving full play to the advantages of both joining methods. Adhesives can alleviate local stress concentration during rivet piercing, while rivets make up for the performance shortcomings of adhesives under high-temperature or impact conditions.

For adhesive-riveted hybrid joints, rivet material design must balance adhesive compatibility and load synergy. Epoxy adhesives (common in automotive/aerospace) are sensitive to acidic oxides, so rivets with neutral surfaces are preferred over rust-prone carbon steel. As Alpendre et al. (2025) showed, 304 stainless steel rivets paired with epoxy adhesives have a 2.5-times longer fatigue life under 10⁶ cycles. For high-strength scenarios like white body doors, Du et al. (2025) proposed gradient hardness rivets to resist compression and adapt to adhesive shrinkage, avoiding stress concentration.

Surface coatings further optimize the adhesive-rivet synergy. Liu et al. (2024) noted in their pre-holing studies that polytetrafluoroethylene coatings reduce adhesive buildup on rivet shanks during piercing, narrowing the fluctuation range of joint shear strength and ensuring process stability. In hygrothermal environments, silane coatings enhance the bonding between rivets and adhesives by repelling moisture, effectively reducing interfacial peeling and maintaining higher energy absorption capacity after aging. For hybrid joints of carbon fiber-reinforced polymer (CFRP) and light alloys, Zhang H. et al. (2023) highlighted that nanoceramic coatings (such as ${\rm TiO_2}$) on rivets minimize CFRP fiber abrasion during piercing, significantly reducing the strength loss of the CFRP layer, which is crucial for preserving the structural integrity of CFRP in lightweight applications.

In terms of rivet layout, Cui et al. (2020) studied CFRP/Al electromagnetic adhesive-riveted joints and found that the shear



strength of joints with 4 rivets in a square array layout is the highest with less weight gain, because a reasonable layout can optimize the adhesive layer thickness distribution and enhance the anti-peel torque. Regarding the interaction between the adhesive layer and the rivet, Du et al. (2025) pointed out through steel-aluminum joint experiments that the position of adhesive layer defects has a significant impact on forming quality and mechanical properties, while the influence of defect area ratio is small.

In addition, Liu et al. (2024) proposed that the pre-holing process can improve the performance of self-piercing adhesive-riveted joints; when the pre-holed diameter of the upper sheet is 3 mm, the peak force and energy absorption of the joint are increased by 12.79% and 35.71% respectively compared with non-holed joints. The reason is that the adhesive flows into the rivet cavity through the hole, increasing the bonding area and mechanical interlocking effect.

4.3.3 Joint performance characterization

Rivets make up for the performance deficiencies of adhesives under extreme conditions such as high temperature, low temperature, and impact. Specifically, when the ambient temperature exceeds the glass transition temperature of the structural adhesive, the adhesive layer will soften, causing its modulus and strength to drop sharply (Zhang H. et al., 2023). In severe cold environments (e.g., -40 °C), the adhesive layer becomes brittle, and its impact resistance deteriorates. At this time, the mechanically interlocked riveting points become the main load transfer path, ensuring that the joint still has a certain residual strength after the adhesive fails. Alpendre et al. (2025) studied highstrength steel sheets and showed that when double-drill riveting is combined with adhesive bonding, regardless of whether riveting is performed before or after adhesive curing, the shear and peel strength of hybrid joints are significantly higher than those of single adhesive or riveted joints. Sadowski et al. (2011) further confirmed through aluminum sheet experiments that the tensile strength of adhesive-riveted hybrid joints is not only higher than that of single adhesive or riveted joints, but also their energy absorption capacity

is significantly improved due to the synergy of the two joining mechanisms. Jiang et al. (2021) studied Al/steel structures and showed that the peak load of joints combining electromagnetic selfpiercing riveting and adhesive bonding is 177.3% higher than that of single riveted joints, and the energy absorption is 360.0% and 47.9% higher than that of single riveting and adhesive bonding respectively; the failure process presents a progressive mode of first adhesive layer failure and then rivet bearing, this staged failure behavior originates from the microscale synergistic deformation between the adhesive layer and the mechanical interlock interface, which delays crack propagation. Ibrahim and Cronin (2022) also tested aluminum alloy joints and showed that the strength of adhesive-riveted hybrid joints with 1-2 mm thick sheets is close to that of single adhesive joints, while the energy absorption is 53.5% higher than that of single self-piercing riveting, taking into account lightweight and fatigue resistance, which is suitable for carrier tool body structures. At the same time, the joint performance of the adhesive-riveted hybrid joining process is affected by various process parameters.

The research on numerical simulation and failure mechanism provides a theoretical basis for process optimization. Gómez et al. (2007) established a mechanical model of adhesive-riveted singlelap joints using Bond-Graph technology, and accurately reproduced the experimental curves through 4 characteristic parameters, providing a simplified method for predicting joint stiffness and strength. Presse et al. (2021) proposed a stress-based fatigue life calculation method for aluminum-high-strength steel hybrid joints, and realized the quantitative evaluation of fatigue performance combined with the material S-N curve. In terms of failure mechanism, Zhang J. et al. (2023) studied Al/CFRP adhesive-riveted joints and showed that the failure process is divided into three stages: the failure proceeds through a sequence of initial adhesiverivet load-sharing, progressive adhesive fracture, and final loadbearing by the rivet alone; temperature has a significant impact on strength, and hygrothermal aging mainly affects the elongation at break. For the connection of CFRP and light alloys, the HH-BR process proposed by Su et al. (2024), which combines pre-holed adhesive bonding and self-piercing riveting, improves the interlock

value between the rivet and the sheet, and the joint strength and energy absorption are better than traditional processes; the failure mode is mainly rivet bending and fiber tearing, reducing brittle fracture caused by insufficient material ductility. The high-speed load experiment by Wen et al. (2024) showed that the peak load of aluminum alloy electromagnetic self-piercing adhesive-riveted joints increases with the speed under dynamic loading, and the rivet remains connected to aluminum when failing, avoiding overall disintegration, which is suitable for the safety design of carrier tools.

4.3.4 Existing problems and future directions

The adhesive-rivet hybrid joining process enables adhesives to disperse the local stress caused by rivet piercing, while rivets make up for the performance shortcomings of adhesives under high temperatures and impact loads—this combination can significantly improve the service life and performance of joints. However, the stress transfer path of adhesive-rivet synergy under dynamic loads, as well as the interfacial hydrolysis of adhesives and the degradation mechanism of joint mechanical interlocking, have not yet been clarified. Moreover, numerical simulations ignore the nonlinear behavior of adhesives, making it difficult to predict performance in extreme environments. Future efforts should focus on three aspects: first, developing high-temperature and moistureheat resistant adhesives; second, establishing a multi-field coupling simulation model; and third, introducing machine vision to achieve real-time monitoring of adhesive layer defects.

4.4 Friction self-piercing riveting

4.4.1 Process principle and flow

Friction Self-Piercing Riveting (F-SPR) is a new solid-state joining technology integrating traditional self-piercing riveting and friction stir processing. As shown in Figure 11c (Ma et al., 2017), the rivet rotates at high speed to contact the surface of the material to be connected, and the local material is softened by frictional heat, which improves the plasticity of low-ductility light alloys; then, under the pressure of the punch, the rivet pierces the upper material and forms a mechanical lock with the lower material; the friction stir effect promotes dynamic recrystallization at the contact surface, forming a solid-state metallurgical bond, and finally realizing the dual strengthening of mechanical interlocking and solid-state joining.

Compared with traditional self-piercing riveting, F-SPR reduces material deformation resistance through frictional heat, which can significantly reduce tool force and avoid brittle fracture of low-ductility materials (Ma et al., 2021).

4.4.2 Key influencing factors and process optimization

Key process parameters, such as frictional heat input and axial pressure, collectively determine the thermo-mechanical cycle in the joining zone, which in turn governs the extent of dynamic recrystallization and the evolution of the microstructure.

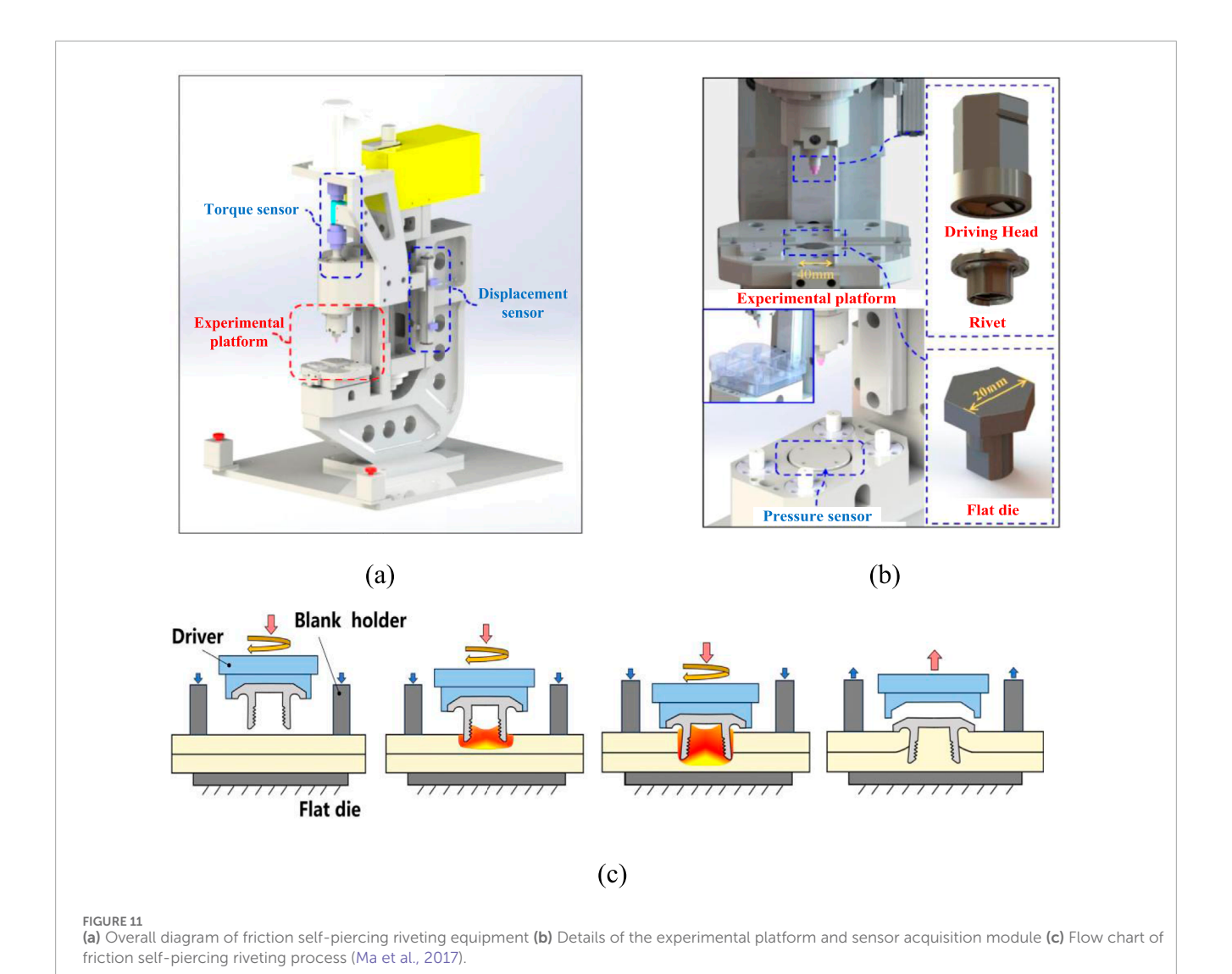
Liu et al. (2016) studied the connection of AA7075-T6 and AZ31B and found that higher rotation speed and slower punch speed can reduce axial force and torque, but reduce the interlock amount between the rivet and the material; at the same time, high

rotation speed promotes local flow of aluminum and magnesium alloys, forming an aluminum layer wrapping the rivet legs. Yang et al. (2022a) used a flat die to connect AA6061-T6 and AZ31B and found that increasing the feed rate reduces frictional heat input, leading to an increase in riveting force, thereby increasing the bottom thickness and interlock amount of the joint, but reducing the material heat-affected zone. In addition, Zhang B. et al. (2024) adjusted the geometry of the stir zone through the design of annular bosses by customizing the rivet structure, increasing the joint strength by 6.9%–11.1%.

4.4.3 Joint performance characterization

Ma et al. (2022) compared F-SPR and SPR joints of AA5182 and found that the former has significantly higher lap shear strength and fatigue life due to the existence of solid-state joining. The underlying reason is that the frictional heat promotes dynamic recrystallization in the interfacial region, resulting in a refined grain structure that enhances the joint's strength and toughness. Li et al. (2022) investigated F-SPR joints between CFRP and AZ31B and found that the fatigue performance under high load was superior to that of resistance spot welding. This enhancement is attributed to the metallurgically bonded zone formed by friction stirring, which effectively suppresses crack propagation. Yuan et al. (2025) further confirmed through fatigue analysis of 2060-T8 aluminum alloy joints that the failure mode under high load is rivet shear + local fracture of the lower material, while under low load, it is the fracture of the lower material at the rivet tip. Stress concentration and fretting wear are key factors. Joint failure is related to the matching of "mechanical interlock strength - solid-state joining strength - local material performance." For example, in adhesive-riveted hybrid F-SPR, adhesives reduce the mechanical interlock amount through lubrication, but after baking and curing, they can promote the precipitation of strengthening phases in the heat-affected zone of aluminum alloys, making the shear strength of joints significantly higher than that of pure F-SPR (Yang et al., 2022b).

F-SPR also performs well in the connection of dissimilar lowductility light alloys. The single-sided F-SPR process developed by Xian et al. (2019) reduces the frictional heat of the lower material through a two-stage feeding method, significantly improving the shear strength and transverse tensile strength of AA6061-T6 joints respectively. As an important single-sided connection variant of F-SPR, Single-Sided Friction Self-Piercing Riveting (SSFR) is specifically designed for enclosed or hard-to-reach areas (e.g., aircraft cabins, closed automotive chassis components), addressing the applicability limitations of traditional double-sided F-SPR. It achieves the full process of "frictional softening - piercing - interlocking" with only single-sided force application through optimized tooling structures and process strategies. Zhang Z. et al. (2024) increased the shear strength of AA7075-T6/DP590 dissimilar joints by 6.9%-11.1% compared to conventional single-sided F-SPR by designing annular boss structures in SSFR to regulate the stir zone geometry, while reducing the risk of brittle phase formation at the interface. In terms of process mechanism, Bingxin et al. (2023) revealed via thermo-mechanical coupling simulation that the single-end dynamic loading of SSFR concentrates the material strain rate in the riveting region, promoting dynamic recrystallization of low-ductility AZ31B magnesium alloy and refining its grain size to 1-2 μm, thereby improving joint fatigue



life. Ma et al. (2017) verified SSFR's applicability in aluminum alloy/composite connections in early feasibility studies, resolving insufficient interlocking caused by single-sided operation by adjusting the matching relationship between rivet rotation speed and axial pressure. Recent research has further focused on extreme service conditions: Yuan et al. (2025) showed that after 720 h of salt spray corrosion, the residual shear strength of SSFR joints

remains above 65% of the base material, outperforming traditional double-sided F-SPR. For process parameter optimization, Yu et al. (2025) optimized SSFR's rotation speed (1,500–2,500 r/min) and feed rate (2–5 mm/s) using response surface methodology, establishing a quantitative model between joint strength and process parameters to support large-scale applications. In addition, the ratio of mechanical interlocking and solid-state joining can be

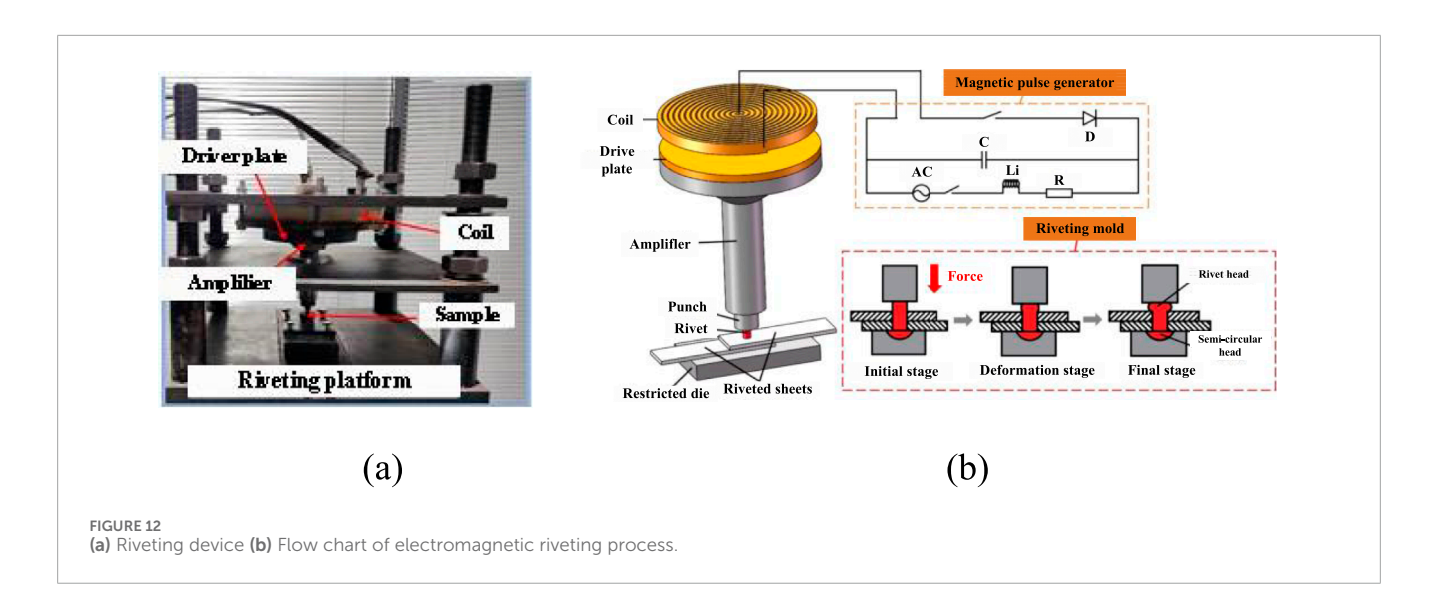
ratio of mechanical interlocking and solid-state joining can be quantitatively controlled by optimizing process parameters through numerical simulation, providing accurate guidance for engineering applications (Ma et al., 2020).

The microstructure directly affects the performance of F-SPR joints. Low-ductility materials undergo dynamic recrystallization under the action of frictional heat and mechanical force. For

example, an ultra-fine grain structure is formed at the AZ31B magnesium alloy joint, which significantly improves the hardness; in AA7075-T6 joints, the aluminum captured in the rivet cavity forms a solid-state joining zone with the lower aluminum sheet through dynamic recrystallization, whose yield strength reaches 75% of the base material and elongation exceeds that of the base material (Ma et al., 2022). In the connection of dissimilar materials, a composite joining layer is easily formed at the interface, and the influence of interface products on joining strength needs to be regulated through parameter optimization (Shan et al., 2023). The threaded rivet FSRW by Zhang P. et al. (2022) increases the shear and transverse tensile strength of joints by 65% and 170% respectively compared with friction stir spot welding. Therefore, regarding the influence of process parameters on joint forming quality and performance.

4.4.4 Existing problems and future directions

F-SPR has broken through the technical bottleneck in joining low-ductility lightweight alloys via the synergistic regulation of thermal-mechanical-metallurgical effects. Its characteristics of high



joining efficiency and strong material adaptability have made it one of the key joining technologies for lightweight structures of transportation vehicles. Although current research has clarified the strength-enhancing effect of DRX, it has not yet defined the relationship between grain size, dislocation density, and solid-state joining strength. Numerical simulation fails to quantify the thermal-mechanical-metallurgical coupling effect, making it difficult to predict the evolution of interfacial products. Future research should, first, establish a correlation model between frictional heat and microstructure by integrating technologies such as EBSD; second, optimize joint performance through rivet surface coating; third, develop a multi-field coupling simulation platform; and finally, advance equipment miniaturization to reduce mass production costs.

4.5 Electromagnetic riveting

4.5.1 Process principle and flow

Electromagnetic Riveting (EMR) is an advanced process for material joining based on the principle of electromagnetic induction. It generates instantaneous impact force through the electromagnetic repulsion between the coil and the driver plate to plasticize the rivet, thereby completing the connection, as shown in Figure 12b. Its unique dynamic loading characteristics make it show significant advantages in the joining of low-ductility light alloy materials, and it has become one of the key technologies for the assembly of lightweight structures of carrier tools (Cao and Zuo, 2020).

4.5.2 Key influencing factors and process optimization

Compared with traditional riveting processes, the core advantages of EMR are reflected in two aspects: microstructure regulation and mechanical property improvement. The core process characteristic of high-strain-rate dynamic loading significantly influences the material's plastic deformation mechanism and microstructural evolution.

Gong et al. (2021) established a numerical model of electromagnetic repulsion force based on circuit, electromagnetism and dynamics theories, which can calculate parameters such as current, impact force and rivet deformation, providing a basis for process parameter optimization. Aiming at the low energy conversion efficiency of traditional induction electromagnetic riveting, Hu et al. (2025) applied a new reluctance electromagnetic riveting (REMR), which can achieve higher energy conversion efficiency at low voltage; when riveting 2A10 aluminum alloy rivets, the voltage is lower than that of the traditional process, the efficiency is increased by 156%, and the adiabatic shear band is narrower. In terms of expanding the connection of dissimilar materials, Jin et al. (2025) applied the flat electromagnetic self-piercing riveting process and used new semi-solid rivets, reducing the CFRP damage in the connection of carbon fiber reinforced plastics and 5052 aluminum alloys through rivet shank upsetting and secondary expansion of rivet legs, with the peak load increased by 18.3%. The construction of theoretical models has further improved the application basis of EMR. Zhang et al. (2019) constructed an interference fit model based on stress wave theory and thick-walled cylinder theory, comprehensively considering parameters such as material properties, geometric dimensions and riveting force, predicted the residual stress distribution, and provided scientific guidance for process design.

4.5.3 Joint performance characterization

Study on 2A10 and 6082 aluminum alloys revealed that the grain deformation in the shear zone of the EMR-driven head is more severe, and the interference distribution is more uniform. This homogeneous microscopic deformation is attributed to more sufficient dislocation slip and grain refinement under the high-energy impact, thereby enhancing the fatigue performance of the joint (Dong et al., 2019). Wang Y. et al. (2023) found in the riveting of TB2 titanium alloy that the interference amount of EMR joints is not only larger than that of hot riveting but also more uniform; the deformation of the driver head and rivet shank is more significant, and the hardness is higher; at the same time, the mechanical

properties of the joint are not reduced, which can effectively replace the hot riveting process.

For titanium alloy rivets, EMR can realize efficient joining of hard-to-deform materials at room temperature; the average relative interference amount of multi-layer structures reaches 2.5%-3.0%, the shear load of the rivet tail reaches 9.9 kN, and the pull-out load reaches 12.5 kN (Zhang et al., 2018). In terms of mechanical properties, the fatigue resistance of EMR joints is particularly prominent. Under shear load, the fatigue life of EMR joints is 1-3 times that of conventional pressure riveted joints, and the fatigue crack growth zone is wider under low cycle stress Li et al. (2017); Jiang et al. (2019) found that when using an 80° special rivet die, the pull-out fatigue life of EMR joints is significantly higher than that of flat dies, because the special die limits the radial flow of the rivet head material and increases the interference fit strength. In the connection of Al/high-strength steel DP590 dissimilar materials, there are two fatigue failure modes for electromagnetic high-speed nailed joints; with 253 MPa as the critical stress, the rivet shank fractures under high stress, and the rivet head fractures under low stress (Jiang et al., 2022). In addition, prefabricated cracks have a special impact on the performance of EMR joints; the shear bearing capacity of 2A10 aluminum alloy rivet joints with prefabricated cracks is slightly higher than that of joints without cracks, but the failure displacement of joints without cracks is larger, and the vibration reduction effect is better (Zhang et al., 2025b).

4.5.4 Existing problems and future directions

In summary, electromagnetic riveting, by virtue of the dynamic loading characteristics of instantaneous high strain rate, can not only promote more uniform plastic deformation of low-ductility light alloys during joining but also improve the overall performance of joints by regulating the material microstructure. The deep integration of numerical simulation technology and electromagnetic riveting provides precise guidance for process parameter optimization. This technical synergy not only expands the application boundary of electromagnetic riveting in lightweight structures of carrier tools but also provides a solid guarantee for connection reliability under complex working conditions.

5 Conclusion

This section is not mandatory but can be added to the manuscript if the discussion is unusually long or complex.

Driven by the global "dual carbon" goals and strict emission regulations, lightweight of carrier tools has become the core direction of industry development. Low-ductility light alloys, with high specific strength and low density, are key to achieving material lightweight. However, in actual connection applications, traditional fusion welding technology is difficult to meet the joining requirements of dissimilar materials and low-ductility materials due to problems such as brittle phase formation, thermal deformation and galvanic corrosion caused by high temperature. Riveting, as an efficient cold joining technology, has become an important solution.

This paper systematically reviews the research progress of riveting processes for low-ductility light alloys. In terms of traditional technologies: solid rivet riveting improves the

deformation uniformity and connection reliability of lowductility materials through the collaborative optimization of rivet geometric parameters and process parameters; blind rivet riveting effectively suppresses material brittle fracture by regulating the balance between mandrel tension and deformation rate, expanding the application of single-sided operation scenarios. In terms of new joining processes: self-piercing riveting (SPR) reduces material damage by virtue of the pre-opening-free characteristic, and die optimization further improves interlock quality and joint performance; pre-holed self-piercing riveting (PH-SPR) significantly enhances the bearing capacity of multilayer dissimilar material joints by optimizing the mechanical interlock structure through preset hole diameters; adhesive-riveted hybrid joining greatly improves the static load strength, fatigue life and environmental adaptability of joints by using the synergistic effect of adhesives and rivets; friction self-piercing riveting (F-SPR) realizes the dual strengthening of "mechanical interlocking - solid-state joining" by softening materials through frictional heat and promoting dynamic recrystallization, effectively solving the cracking problem of low-ductility alloys; electromagnetic riveting (EMR) promotes uniform plastic deformation of materials through high strain rate dynamic loading, showing unique advantages in the joining of hard-to-deform materials such as titanium alloys. In conclusion, the riveting process is undergoing an evolution from traditional parameter optimization towards innovative mechanisms that integrate thermal energy and high-energy fields, thereby enhancing joint reliability.

However, numerous unresolved challenges and technical bottlenecks persist in both traditional and novel riveting processes for low-ductility light alloys: at the material level, uneven plastic flow is prone to cause local stress concentration and crack initiation, and the influence mechanism of residual stress on long-term service performance is not clear; at the process level, parameter optimization of new processes (such as F-SPR) mostly relies on experimental trial and error, lacking accurate control models for thermal-force-metallurgy multi-field coupling; in terms of performance evaluation, research on the performance degradation law of joints under complex working conditions (corrosion, impact, fatigue, high temperature) is insufficient, and the prediction accuracy of unique brittle failure modes of low-ductility materials is limited; at the engineering application level, problems such as galvanic corrosion protection of dissimilar materials, cost-benefit balance of new processes and adaptability to large-scale production need to be solved urgently.

To overcome the application bottlenecks of low-ductility lightweight alloy riveting in the future, research must transition from an "empirical trial-and-error" approach to a "model-driven" paradigm. Breakthroughs should be pursued along the following key pathways: First, to overcome the limitation of relying on experimental methods for process parameter optimization due to the lack of precise theoretical foundations, an intelligent riveting system based on digital twins and machine learning should be developed. By integrating multi-physics simulations and data-driven algorithms, real-time prediction and adaptive control of process parameters can be achieved, fundamentally enhancing the consistency of forming quality. Second, to tackle the challenge of synergizing mechanical, corrosion, and fatigue properties in joints of dissimilar materials, multi-functional hybrid processes

such as adhesive-riveting and electromagnetic-friction techniques should be explored. Through the use of smart rivets and integrated structural-functional design, the joint load-bearing capacity and durability can be synergistically improved. Regarding the issue of inaccurate service performance prediction of joints under complex working conditions, full lifecycle performance evaluation, reliability management, and online monitoring technologies should be adopted. These approaches will enable accurate prediction of joint lifespan, providing a scientific basis for the safe operation and maintenance of transport vehicles. The coordinated advancement of these pathways will significantly enhance the ability of riveting technology to support the high-quality, lightweight development of transport vehicles.

Author contributions

ZD: Methodology, Funding acquisition, Writing – review and editing. SR: Investigation, Data curation, Writing – original draft. BM: Project administration, Writing – review and editing, Methodology. XM: Data curation, Investigation, Writing – review and editing. LR: Formal Analysis, Writing – review and editing, Conceptualization. LX: Writing – review and editing, Resources, Visualization. FY: Validation, Methodology, Writing – review and editing. DY: Writing – original draft, Data curation. CC: Data curation, Writing – original draft.

Funding

The author(s) declare that financial support was received for the research and/or publication of this article. The work is supported from Jiangsu Provincial Key Research and Development Program (BE2022053-4) and Natural Science Foundation of Jiangsu Province (grant number BK20230530). China Postdoctoral Science

References

Adade, S. Y.-S. S., Lin, H., Haruna, S. A., Johnson, N. A. N., Barimah, A. O., Afang, Z., et al. (2024). Multicomponent prediction of Sudan dye adulteration in crude palm oil using SERS – based bimetallic nanoflower combined with genetic algorithm. *J. Food Compos. Analysis* 125 (Suppl. C), 105768. doi:10.1016/j.jfca.2023.105768

Ali, K. H., Nafey, Z., Asad, H., Farooq, A., Kamran, A., Saad, J., et al. (2022). Development and characterization of a new riveting process for pre-drilled holes hard-to-access aircraft riveted joints. *Int. J. Adv. Manuf. Technol.* 120 (9-10), 6635–6646. doi:10.1007/s00170-022-09167-3

Alpendre, J. M. B., Rosado, P. M. S., Sampaio, R. F. V., Pragana, J. P. M., Bragança, I. M. F., Silva, C. M. A., et al. (2025). Enhancing the performance of double-flush riveted joints through hybridization with adhesive bonding. *J. Adv. Join. Process.* 12, 100324. doi:10.1016/j.jajp.2025.100324

Anonymous (2023). "Global light vehicle materials market - forecasts to 2035: 2023," in PESTER analysis. Just - Auto. Q2 Edition, 2–5.

Arslan, M., Zou, X. B., Tahir, H. E., Xuetao, H., Rakha, A., Basheer, S., et al. (2018). Near-infrared spectroscopy coupled chemometric algorithms for prediction of antioxidant activity of black goji berries (Lycium ruthenicum Murr.). *J. Food Meas. Charact.* 12 (4), 2366–2376. doi:10.1007/s11694-018-9853-x

Arslan, M., Zou, X. B., Tahir, H. E., Hu, X. T., Rakha, A., Zareef, M., et al. (2019). NIR spectroscopy coupled chemometric algorithms for rapid antioxidants activity assessment of Chinese dates (Zizyphus Jujuba Mill.). *Int. J. Food Eng.* 15 (3-4), 20180148. doi:10.1515/ijfe-2018-0148

Bai, J., Yang, Y., Wen, C., Chen, J., Zhou, G., Jiang, B., et al. (2023). Applications of magnesium alloys for aerospace: a review. *J. Magnesium Alloys* 11 (10), 3609–3619. doi:10.1016/j.jma.2023.09.015

Foundation (grant number 2024M751166). Basic Research Special Fund of Jiangsu Province (Major Innovation Platforms Program) (SBM2024110013).

Conflict of interest

Authors SR, BM, XM, LR, and LX were employed by Chery Automobile Co., Ltd. Authors FY, DY, and CC were employed by Suzhou Swangsea Intelligent Equipment Technology Co., Ltd.

The remaining author declares that the research was conducted in the absence of any commercial or financial relationships that could be construed as a potential conflict of interest.

Generative AI statement

The author(s) declare that no Generative AI was used in the creation of this manuscript.

Any alternative text (alt text) provided alongside figures in this article has been generated by Frontiers with the support of artificial intelligence and reasonable efforts have been made to ensure accuracy, including review by the authors wherever possible. If you identify any issues, please contact us.

Publisher's note

All claims expressed in this article are solely those of the authors and do not necessarily represent those of their affiliated organizations, or those of the publisher, the editors and the reviewers. Any product that may be evaluated in this article, or claim that may be made by its manufacturer, is not guaranteed or endorsed by the publisher.

Bingxin, Y., Yunwu, M., He, S., and Yongbing, L. (2023). A comparative study of selfpiercing riveting and friction self-piercing riveting of cast aluminum alloy Al–Si7Mg. *J. Manuf. Sci. Eng.* 145 (1), 011003. doi:10.1115/1.4055324

Bonah, E., Huan, X. Y., Yi, R., Aheto, J. H., Osae, R., and Golly, M. (2019). Electronic nose classification and differentiation of bacterial foodborne pathogens based on support vector machine optimized with particle swarm optimization algorithm. *J. Food Process Eng.* 42 (6), e13236. doi:10.1111/jfpe.13236

Borba, N. Z., Blaga, L., Santos, J. F. d., and Amancio-Filho, S. T. (2018). Direct-friction Riveting of polymer composite laminates for aircraft applications. *Mater. Lett.* 215, 31–34. doi:10.1016/j.matlet.2017.12.033

Bothiraj, T., Saravanan, M., Srinivasan, R., and Tharmalingam, S. (2023). Optimization of friction stir blind riveting process parameters for non-ferrous sheet metal alloys. *Mater. Today Proc.* 74, 26–33. doi:10.1016/j.matpr. 2022 10 007

Cacko, R. (2008). Review of different material separation criteria in numerical modeling of the self-piercing riveting process – SPR. *Archives Civ. Mech. Eng.* 8 (2), 21–30. doi:10.1016/s1644-9665(12)60190-3

Cao, Z., and Zuo, Y. (2020). Electromagnetic riveting technique and its applications. *Chin. J. Aeronautics* 33 (1), 5–15. doi:10.1016/j.cja.2018.12.023

Cao, H., Zhang, Q., Zhu, W., Cui, S., Yang, Q., Wang, Z., et al. (2024). Study on the influence of injection velocity on the evolution of hole defects in die-cast aluminum alloy. *Materials* 17 (20), 4990. doi:10.3390/ma17204990

Casarotto, F., Franke, A. J., and Franke, R. (2012). "6 - high-pressure die-cast (HPDC) aluminium alloys for automotive applications," in *Advanced materials in automotive*

- engineering. Editor J. Rowe (Cambridge, UK; Philadelphia, PA, USA: Woodhead Publishing), 109–149. doi:10.1533/9780857095466.109
- Chai, X., Xu, L., Sun, Y., Liang, Z., Lu, E., and Li, Y. (2020). Development of a cleaning fan for a rice combine harvester using computational fluid dynamics and response surface methodology to optimise outlet airflow distribution. *Biosyst. Eng.* 192 (No.0), 232–244. doi:10.1016/j.biosystemseng.2019.12.016
- Chen, H.-C., Pinkerton, A. J., and Li, L. (2011). Fibre laser welding of dissimilar alloys of Ti-6Al-4V and Inconel 718 for aerospace applications. *Int. J. Adv. Manuf. Technol.* 52 (9-12), 977–987. doi:10.1007/s00170-010-2791-3
- Chen, S., Zhou, Y., Tang, Z., and Lu, S. (2020). Modal vibration response of rice combine harvester frame under multi-source excitation. *Biosyst. Eng.* 194, 177–195. doi:10.1016/j.biosystemseng.2020.04.002
- Chen, G., Zeng, K., Xing, B., and He, X. (2022). Multiple nonlinear regression prediction model for process parameters of Al alloy self-piercing riveting. *J. Mater. Res. Technol.* 19, 1934–1943. doi:10.1016/j.jmrt.2022.05.118
- Chen, X., Chen, R., Wang, J., Li, H., and Zhang, W. (2024a). Evaluation of water distribution and uniformity of sprinkler irrigation based on harmonic analysis and finite element method. *Biosyst. Eng.* 248, 308–320. doi:10.1016/j.biosystemseng.2024.11.010
- Chen, X., Zhang, J., Wang, M., Wang, W., Zhao, D., Huang, H., et al. (2024b). Research progress of heterogeneous structure magnesium alloys: a review. *J. Magnesium Alloys* 12 (6), 2147–2181. doi:10.1016/j.jma.2024.04.001
- Chen, J., Wang, B., Zhang, Y., Zhang, Z., Wei, Q., Wu, W., et al. (2025). Corrosion behavior and mechanical performance of AZ31/PEEK joints fabricated by friction stir spot joining and self-piercing riveting. CIRP J. Manuf. Sci. Technol. 61, 296–307. doi:10.1016/j.cirpj.2025.06.018
- Cui, J., Gao, S., Jiang, H., Huang, X., Lu, G., and Li, G. (2020). Adhesive bond-electromagnetic rivet hybrid joining technique for CFRP/Al structure: process, design and property. *Compos. Struct.* 244, 112316. doi:10.1016/j.compstruct.2020.112316
- Cui, J., Sun, H., Jing, L., Sun, L., Li, G., and Jiang, H. (2022). Failure analysis of pulse magnetic induction coil in electromagnetic riveting. *Eng. Fail. Anal.* 136, 106178. doi:10.1016/j.engfailanal.2022.106178
- Danyo, M. W. (2014). "10 self-piercing riveting (SPR) in the automotive industry: an overview," in *Self-piercing riveting*. Editors A. Chrysanthou, and X. Sun (Cambridge, UK: Woodhead Publishing), 171–180. doi:10.1533/9780857098849.2.171
- Ding, Z., Tang, Z., Zhang, B., and Ding, Z. (2024). Vibration response of metal plate and shell structure under multi-source excitation with welding and bolt connection. *Agriculture* 14 (6), 816. doi:10.3390/agriculture14060816
- Dong, D., Sun, L., Wang, Q., Li, G., and Cui, J. (2019). Influence of electromagnetic riveting process on microstructures and mechanical properties of 2A10 and 6082 Al riveted structures. *Archives Civ. Mech. Eng.* 19 (4), 1284–1294. doi:10.1016/j.acme.2019.07.006
- Dong, J., Jiang, J., Wang, Y., Qin, T., Huang, M., Cui, J., et al. (2025). Research on numerical simulation and integrated die casting process of large complex thin-walled aluminum alloy automobile rear floor. *Results Eng.* 26, 105399. doi:10.1016/j.rineng.2025.105399
- Du, Z., Duan, L., Jing, L., Cheng, A., and He, Z. (2021a). Numerical simulation and parametric study on self-piercing riveting process of aluminium–steel hybrid sheets. *Thin-Walled Struct.* 164, 107872. doi:10.1016/j.tws.2021.107872
- Du, Z., Wei, B., He, Z., Cheng, A., Duan, L., and Zhang, G. (2021b). Experimental and numerical investigations of aluminium–steel self-piercing riveted joints under quasi-static and dynamic loadings. *Thin-Walled Struct.* 169, 108277. doi:10.1016/j.tws.2021.108277
- Du, Z., Duan, L., Ma, B., Ren, L., Meng, X., Xu, L., et al. (2025). Experimental and numerical investigations on process-performance for steel-aluminum riv-bonding joints. *Eng. Fail. Anal.* 177, 109666. doi:10.1016/j.engfailanal.2025.109666
- Duan, J., and Chen, C. (2023). Effect of edge riveting on the failure mechanism and mechanical properties of self-piercing riveted aluminium joints. *Eng. Fail. Anal.* 150, 107305. doi:10.1016/j.engfailanal.2023.107305
- Duan, L., Du, Z., Ma, H., Li, W., Xu, W., and Liu, X. (2023). Simplified modelling of self-piercing riveted joints and application in crashworthiness analysis for steel-aluminium hybrid beams. *J. Manuf. Process.* 85, 948–962. doi:10.1016/j.jmapro.2022.11.068
- El-Emam, M. A., Zhou, L., and Omara, A. I. (2023). Predicting the performance of aero-type cyclone separators with different spiral inlets under macroscopic bio-granular flow using CFD-DEM modelling. *Biosyst. Eng.* 233, 125–150. doi:10.1016/j.biosystemseng.2023.08.003
- Felix, H., Karina, N., Thomas, N., Normen, F., Michael, R., and Knuth-Michael, H. (2023). Design of aluminium solid self-piercing rivets for joining aluminium sheets by material and geometric modification. *J. Adv. Join. Process.* 8, 100161. doi:10.1016/j.jajp.2023.100161
- Feng, J., Zhang, J., Jin, W., and Liao, R. (2024). Damage evolution modeling of CFRP/Al single-lap screw type blind riveted joints during realistic installation process. *Compos. Struct.* 337, 118023. doi:10.1016/j.compstruct.2024.118023

- Fordjour, A., Zhu, X., Yuan, S., Dwomoh, F. A., and Issaka, Z. (2020). Numerical simulation and experimental study on internal flow characteristic in the dynamic fluidic sprinkler. *Appl. Eng. Agric.* 36 (1), 61–70. doi:10.13031/aea.13624
- Gómez, S., Oñoro, J., and Pecharromán, J. (2007). A simple mechanical model of a structural hybrid adhesive/riveted single lap joint. *Int. J. Adhesion Adhesives* 27 (4), 263–267. doi:10.1016/j.ijadhadh.2006.01.004
- Gong, C., Fan, Z., Cheng, L., and Deng, J. (2021). Predictions of the total electromagnetic repulsion force in electromagnetic riveting process: numerical analysis model and experiments. *J. Manuf. Process.* 69, 656–670. doi:10.1016/j.jmapro.2021.08.022
- Grimm, T., and Drossel, W.-G. (2019). Process development for self-pierce riveting with solid formable rivet of boron steel in multi-material design. *Procedia Manuf.* 29, 271–279. doi:10.1016/j.promfg.2019.02.138
- Guo, Q., Zabed, H., Zhang, H., Wang, X., Yun, J., Zhang, G., et al. (2019). Optimization of fermentation medium for a newly isolated yeast strain (Zygosaccharomyces rouxii JM-C46) and evaluation of factors affecting biosynthesis of D-arabitol. *LWT* 99 (No.0), 319–327. doi:10.1016/j.lwt.2018.09.086
- Guo, Z. M., Wang, M. M., Wu, J. Z., Tao, F. F., Chen, Q. S., Wang, Q. Y., et al. (2019). Quantitative assessment of zearalenone in maize using multivariate algorithms coupled to raman spectroscopy. *Food Chem.* 286, 282–288. doi:10.1016/j.foodchem.2019.02.020
- Heidrich, D., Zhang, F., and Fang, X. (2021). Fatigue strength of rivet resistance spot welding technique in comparison with self-piercing riveting for multi-material body-in-white structure. *J. Mater. Eng. Perform.* 30 (5), 3806–3821. doi:10.1007/s11665-021-05684-6
- Hu, W. W., He, R. H., Hou, F. R., Ouyang, Q., and Chen, Q. S. (2017). Real-time monitoring of alcalase hydrolysis of egg white protein using near infrared spectroscopy technique combined with efficient modeling algorithm. *Int. J. Food Prop.* 20 (7), 1488–1499. doi:10.1080/10942912.2016.1212876
- Hu, Q., Cao, Z., Zhang, M., Wang, J., Gong, X., Guo, Y., et al. (2025). A novel reluctance electromagnetic riveting process: multi-field coupling numerical and experimental studies. *J. Manuf. Process.* 134, 207–220. doi:10.1016/j.jmapro.2024.12.068
- Huang, Z., Zhang, Y., Jiang, Y., and Ma, N. (2024). Formability analysis of self-piercing riveted dissimilar joint of B1500HS steel and AA5052 aluminum alloy. *Mater. Today Commun.* 41, 111038. doi:10.1016/j.mtcomm.2024.111038
- Ibrahim, A. H., and Cronin, D. S. (2022). Mechanical testing of adhesive, self-piercing rivet, and hybrid jointed aluminum under tension loading. *Int. J. Adhesion Adhesives* 113, 103066. doi:10.1016/j.ijadhadh.2021.103066
- Jacek, M. (2013). The effect of material properties and joining process parameters on behavior of self-pierce riveting joints made with the solid rivet. *Mater. Des.* 52,932-946. doi:10.1016/j.matdes.2013.06.037
- Järvikivi, M. (2021). The road to automotive lightweighting. *Ind. Heat.* 89 (6), 38–40. Available at: https://www.proquest.com/scholarly-journals/road-automotive-light-weighting/docview/2422405287/se-2.
- Jiang, Y., Li, H., Xiang, Q. J., and Chen, C. (2017). Comparison of PIV experiment and numerical simulation on the velocity distribution of intermediate pressure jets with different nozzle parameters. *Irrigation Drainage* 66 (4), 510–519. doi:10.1002/ird.2133
- Jiang, H., Cong, Y., Zhang, J., Wu, X., Li, G., and Cui, J. (2019). Fatigue response of electromagnetic riveted joints with different rivet dies subjected to pull-out loading. *Int. J. Fatigue* 129, 105238. doi:10.1016/j.ijfatigue.2019.105238
- Jiang, H., Liao, Y., Gao, S., Li, G., and Cui, J. (2021). Comparative study on joining quality of electromagnetic driven self-piecing riveting, adhesive and hybrid joints for Al/steel structure. *Thin-Walled Struct.* 164, 107903. doi:10.1016/j.tws.2021.107903
- Jiang, H., Li, B., Li, G., and Cui, J. (2022). Failure behavior of electromagnetic driven nailing riveted joint for Al/steel structures subjected to fatigue loading. *Eng. Fail. Anal.* 132, 105941. doi:10.1016/j.engfailanal.2021.105941
- Jin, J., Yang, W., Liao, Y., Li, G., Cui, J., and Jiang, H. (2024). Fatigue performance of electromagnetic self-pierce riveting-bonding hybrid joint under alternating load and corrosion coupling conditions. *Int. J. Fatigue* 180, 108079. doi:10.1016/j.ijfatigue.2023.108079
- Jin, J., Qin, J., Xu, Y., Li, G., Cui, J., and Jiang, H. (2025). Novel rivet in flat electromagnetic self-piercing riveting with no concave die of CFRP/aluminum structures for enhancing performance. *J. Manuf. Process.* 148, 160–172. doi:10.1016/j.jmapro.2025.05.030
- Jovan, T., and Seeram, R. (2021). Applications of magnesium and its alloys: a review. *Appl. Sci.* 11 (15), 6861. doi:10.3390/app11156861
- Khulal, U., Zhao, J. W., Hu, W. W., and Chen, Q. S. (2016). Nondestructive quantifying total volatile basic nitrogen (TVB-N) content in chicken using hyperspectral imaging (HSI) technique combined with different data dimension reduction algorithms. *Food Chem.* 197, 1191–1199. doi:10.1016/j.foodchem.2015.11.084
- Kim, K.-Y., Sim, J., Jannat, N.-E., Ahmed, F., and Ameri, S. (2019). Challenges in riveting quality prediction: a literature survey. *Procedia Manuf.* 38, 1143–1150. doi:10.1016/j.promfg.2020.01.203
- Kutsanedzie, F. Y. H., Chen, Q. S., Hassan, M. M., Yang, M. X., Sun, H., and Rahman, M. H. (2018). Near infrared system coupled chemometric algorithms for

- enumeration of total fungi count in cocoa beans neat solution. Food Chem. 240, 231–238. doi:10.1016/j.foodchem.2017.07.117
- Li, S., Khan, H., Hihara, L. H., and Li, J. (2016). Marine atmospheric corrosion of Al-Mg joints by friction stir blind riveting. *Corros. Sci.* 111, 793–801. doi:10.1016/j.corsci.2016.05.009
- Li, G., Jiang, H., Zhang, X., and Cui, J. (2017). Mechanical properties and fatigue behavior of electromagnetic riveted lap joints influenced by shear loading. *J. Manuf. Process.* 26, 226–239. doi:10.1016/j.jmapro.2017.02.022
- Li, S., Khan, H. A., Hihara, L. H., Cong, H., and Li, J. (2018). Corrosion behavior of friction stir blind riveted Al/CFRP and Mg/CFRP joints exposed to a marine environment. *Corros. Sci.* 132, 300–309. doi:10.1016/j.corsci.2018.01.005
- Li, Y. T., Sun, J., Wu, X. H., Lu, B., Wu, M. M., and Dai, C. X. (2019). Grade identification of tieguanyin tea using fluorescence hyperspectra and different statistical algorithms. *J. Food Sci.* 84 (8), 2234–2241. doi:10.1111/1750-3841.14706
- Li, Y., Xu, L. Z., Gao, Z. P., Lu, E., and Li, Y. M. (2021). Effect of vibration on rapeseed header loss and optimization of header frame. *Trans. ASABE* 64 (4), 1247–1258. doi:10.13031/trans.13299
- Li, Y., Lim, Y. C., Chen, J., Jun, J., and Feng, Z. (2022). Mechanical joint performances of friction self-piercing riveted carbon fiber reinforced polymer and AZ31B Mg alloy. *J. Magnesium Alloys* 10 (12), 3367–3379. doi:10.1016/j.jma.2022.09.015
- Li, S. S., Yue, X., Li, Q. Y., Peng, H. L., Dong, B. X., Liu, T. S., et al. (2023). Development and applications of aluminum alloys for aerospace industry. *J. Mater. Res. Technol.* 27, 944–983. doi:10.1016/j.jmrt.2023.09.274
- Li, Y., Lim, Y. C., and Feng, Z. (2024). Effect of die design on microstructure and mechanical joint strength in friction self-piercing riveted AA7055-T76 and AA7055-T76. *J. Manuf. Process.* 124, 119–130. doi:10.1016/j.jmapro. 2024.06.005
- Liang, Z., Li, J., Liang, J., Shao, Y., Zhou, T., Si, Z., et al. (2022). Investigation into experimental and DEM simulation of guide blade optimum arrangement in multi-rotor combine harvesters. *Agriculture* 12 (3), 435. doi:10.3390/agriculture12030435
- Liu, B., Yang, J., Zhang, X., Yang, Q., Zhang, J., and Li, X. (2023). Development and application of magnesium alloy parts for automotive OEMs: a review. *J. Magnesium Alloys* 11 (1), 15–47. doi:10.1016/j.jma.2022.12.015
- Liu, X., Lim, Y. C., Li, Y., Tang, W., Ma, Y., Feng, Z., et al. (2016). Effects of process parameters on friction self-piercing riveting of dissimilar materials. *J. Mater. Process. Technol.* 237, 19–30. doi:10.1016/j.jmatprotec.2016.05.022
- Liu, G., Dang, K., Wang, K., and Zhao, J. (2020). Progress on rapid hot gas forming of titanium alloys: mechanism, modelling, innovations and applications. *Procedia Manuf.* 50, 265–270. doi:10.1016/j.promfg.2020.08.049
- Liu, J., Xue, Z., Yu, B., Sun, L., Xu, C., and Li, L. (2024). Influence of predrilled holes in the upper sheets on the formability and bearing capacity of self-piercing riveted bonded structural components. *Mater. Today Commun.* 41, 110584. doi:10.1016/j.mtcomm.2024.110584
- Liu, H., Liu, Z., Deng, T., Yang, Z., Ai, R., Yang, Y., et al. (2025). Enhanced corrosion resistance of near β titanium alloy by deep cryogenic treatment. *Corros. Sci.* 255, 113131. doi:10.1016/j.corsci.2025.113131
- Liu, J. P., Hussain, Z., Wang, X. J., and Li, Y. F. (2023). Optimization and numerical simulation of the internal flow field of water-pesticide integrated microsprinklers. *Irrigation Drainage* 72 (2), 328–342. doi:10.1002/ird.2789
- Lu, Y., Yao, H., Li, C., Han, J., Tan, Z., and Yan, Y. (2016). Separation, concentration and determination of trace chloramphenicol in shrimp from different waters by using polyoxyethylene lauryl ether-salt aqueous two-phase system coupled with high-performance liquid chromatography. *FOOD Chem.* 192 (No.0), 163–170. doi:10.1016/j.foodchem.2015.06.086
- Lu, Y., Liu, Q., Zhang, Z., Qin, L., and Li, Q. (2023). Experimental and numerical investigation into tensile and cross tensile responses of CFRP/Al blind riveted-bonded hybrid joints. *Compos. Struct.* 318, 117077. doi:10.1016/j.compstruct.2023.117077
- Lun, Z., Monier, A., Zhang, A., Li, L., Elkaseer, A., Abbas, Z., et al. (2025). Effects of die type on mechanical performance and failure behaviors of self-piercing riveting joints in AA5052. *J. Mater. Res. Technol.* 35, 4819–4832. doi:10.1016/j.jmrt. 2025.01.243
- Ma, Y., Xian, X., Lou, M., Li, Y., and Lin, Z. (2017). Friction self-piercing riveting (F-SPR) of dissimilar materials. *Procedia Eng.* 207, 950–955. doi:10.1016/j.proeng.2017.10.857
- Ma, Y., Yang, B., Lou, M., Li, Y., and Ma, N. (2020). Effect of mechanical and solid-state joining characteristics on tensile-shear performance of friction self-piercing riveted aluminum alloy AA7075-T6 joints. *J. Mater. Process. Technol.* 278, 116543. doi:10.1016/j.jmatprotec.2019.116543
- Ma, Y., Shan, H., Niu, S., Li, Y., Lin, Z., and Ma, N. (2021). A comparative study of friction self-piercing riveting and self-piercing riveting of aluminum alloy AA5182-O. *Engineering* 7 (12), 1741–1750. doi:10.1016/j.eng.2020.06.015
- Ma, Y., Yang, B., Hu, S., Shan, H., Geng, P., Li, Y., et al. (2022). Combined strengthening mechanism of solid-state bonding and mechanical interlocking in friction self-piercing riveted AA7075-T6 aluminum alloy joints. *J. Mater. Sci. Technol.* 105, 109–121. doi:10.1016/j.jmst.2021.07.026

- Ma, Y., Hu, Y., Yu, Z., Cai, Z., Zheng, W., Yang, J., et al. (2025). Dual-layer TiO₂/PDMS composite coating on Ti6Al4V titanium alloy with superhydrophobicity and enhanced corrosion resistance and mechanical stability. *Surf. Coatings Technol.* 512, 132414. doi:10.1016/j.surfcoat.2025.132414
- Min, J., Li, J., Carlson, B. E., Li, Y., and Lin, J. (2014). Mechanical property of Al alloy joints by friction stir blind riveting. *Procedia Eng.* 81, 2036–2041. doi:10.1016/j.proeng.2014.10.277
- Min, J., Li, J., Li, Y., Carlson, B. E., Lin, J., and Wang, W.-M. (2015a). Friction stir blind riveting for aluminum alloy sheets. *J. Mater. Process. Technol.* 215, 20–29. doi:10.1016/j.jmatprotec.2014.08.005
- Min, J., Li, Y., Carlson, B. E., Hu, S. J., Li, J., and Lin, J. (2015b). A new single-sided blind riveting method for joining dissimilar materials. *CIRP Ann.* 64 (1), 13–16. doi:10.1016/j.cirp.2015.04.047
- Mucha, J. (2014). The numerical analysis of the effect of the joining process parameters on self-piercing riveting using the solid rivet. *Archives Civ. Mech. Eng.* 14 (3), 444–454. doi:10.1016/j.acme.2013.11.002
- Ni, J., Sun, Y., and Ding, W.-x. (2017). Simulation and experiment on the dimensional error for the large-scale assembly linked by abundant solid rivets. *Int. Conf. Appl. Mech. Mech. Automation (AMMA 2017)*. doi:10.12783/dtetr/amma2017/13345
- Pang, J., Li, Y. M., Ji, J. T., and Xu, L. Z. (2019). Vibration excitation identification and control of the cutter of a combine harvester using triaxial accelerometers and partial coherence sorting. *Biosyst. Eng.* 185, 25–34. doi:10.1016/j.biosystemseng.2019.02.013
- Penalva, M., Del Val, A. G., Martín, A., Villanueva, P., Uralde, V., and Veiga, F. (2025). Monitoring of blind rivets installations: contributions from the manufacturing chain and time-series imaging. *Measurement* 254, 117950. doi:10.1016/j.measurement.2025.117950
- Peters, M., Kumpfert, J., Ward, C. H., and Leyens, C. (2003). Titanium alloys for aerospace applications. Adv. Eng. Mater. 5 (6), 419–427. doi:10.1002/adem.200310095
- Ping, X., Zhang, Y., Zhao, H., Liu, Y., Liu, X., Ma, Y., et al. (2025). Performance evaluation of modified refill friction stir riveting process on AA7075-T6 stacks with largely unequal thicknesses. *J. Manuf. Process.* 133, 430–447. doi:10.1016/j.jmapro.2024.11.073
- Presse, J., Künkler, B., and Michler, T. (2021). Stress-based approach for fatigue life calculation of multi-material connections hybrid joined by self-piercing rivets and adhesive. *Thin-Walled Struct*. 159, 107192. doi:10.1016/j.tws.2020.107192
- Qi, S., Wang, C., Liu, Y., Liu, A., Bai, Z., Peng, Z., et al. (2025). Process parameter optimization of laser welding for dissimilar aluminum alloys 4047 and 6061 using response surface methodology: microstructure and mechanical properties. *Opt. Laser Technol.* 190, 113198. doi:10.1016/j.optlastec.2025.113198
- Qin, D., Wang, J., Chen, Y., Lu, R., and Pan, F. (2015). Effect of long period stacking ordered structure on the damping capacities of mg–ni–y alloys. *Mater. Sci. Eng. A* 624, 9–13. doi:10.1016/j.msea.2014.11.011
- Qin, O. Y., Yang, Y. C., Wu, J. Z., Liu, Z. Q., Chen, X. H., Dong, C. W., et al. (2019). Rapid sensing of total theaflavins content in black tea using a portable electronic tongue system coupled to efficient variables selection algorithms. *J. Food Compos. Analysis* 75, 43–48. doi:10.1016/j.jfca.2018.09.014
- Réger, M., Gáti, J., Oláh, F., Horváth, R., Fábián, E. R., and Bubonyi, T. (2023). Detection of porosity in impregnated die-cast aluminum alloy piece by metallography and computer tomography. *Crystals* 13 (7), 1014. doi:10.3390/cryst13071014
- Robert, A.-A., Zhou, C. S., Hafida, W., Abdullateef, T., Muhammad, T. R., Gilbert, S., et al. (2020). Acoustically-aided osmo-dehydration pretreatments under pulsed vacuum dryer for Apple slices: drying kinetics, thermodynamics, and quality attributes. *J. FOOD Sci.* 85 (No.11), 3909–3919. doi:10.1111/1750-3841.15484
- Sadowski, T., Golewski, P., and Zarzeka-Raczkowska, E. (2011). Damage and failure processes of hybrid joints: adhesive bonded aluminium plates reinforced by rivets. *Comput. Mater. Sci.* 50 (4), 1256–1262. doi:10.1016/j.commatsci.2010.06.022
- Samuel, B. I., and Olaf, H. (2010). Simulation of the solid rivet installation process. SAE Int. J. Aerosp. 3 (1), 187–197. doi:10.4271/2010-01-1843
- Shan, H., Ma, Y., Yang, B., Feng, Q., Li, Y., and Lin, Z. (2023). Elucidation of interface joining mechanism of aluminum alloy/dual-phase steel friction stir riveting (FSR) joint. *J. Mater. Res. Technol.* 25, 6792–6811. doi:10.1016/j.jmrt.2023.07.146
- Shen, J., Zhang, Q., and Tian, S. (2025). Impact of the vehicle lightweighting and electrification on the trend of carbon emissions from automotive materials. *J. Clean. Prod.* 513, 145677. doi:10.1016/j.jclepro.2025.145677
- Shi, M., Ruan, Y., Wu, B., Ye, Z., and Zhu, S. (2017). Performance evaluation of hydrodynamic vortex separator at different hydraulic retention times applied in recirculating biofloc technology system. *Trans. ASABE* 60 (No.5), 1737–1747. doi:10.13031/trans.12415
- Shi, Q., Mao, H., and Guan, X. (2019). Numerical simulation and experimental verification of the deposition concentration of an unmanned aerial vehicle. *Appl. Eng. Agric.* 35 (3), 367–376. doi:10.13031/aea.13221
- Silvayeh, Z., Stippich, J., Auer, P., and Domitner, J. (2024). Influence of irregular rivet-die offsets on the integrity and on the load-bearing capacity of self-piercing-riveted aluminum alloy joints. *Procedia Struct. Integr.* 54, 431–436. doi:10.1016/j.prostr.2024.01.103

- Singh, P., Pungotra, H., and Kalsi, N. S. (2017). On the characteristics of titanium alloys for the aircraft applications. *Mater. Today Proc.* 4 (8), 8971–8982. doi:10.1016/j.matpr.2017.07.249
- Stephens, E. V. (2014). "2 mechanical strength of self-piercing riveting (SPR)," in Self-Piercing riveting. Editors A. Chrysanthou, and X. Sun (Cambridge, UK: Woodhead Publishing), 11–32. doi:10.1533/9780857098849.1.11
- Su, H., Deng, K., Yang, D., Zhan, X., Xie, Z., Qin, J., et al. (2024). Performance and failure analysis of perforated CFRP/aluminum alloy bonding and self-piercing riveting hybrid joints. *Eng. Fail. Anal.* 156, 107803. doi:10.1016/j.engfailanal.2023.107803
- Sun, J., Lu, X. Z., Mao, H. P., Wu, X. H., and Gao, H. Y. (2017). Quantitative determination of rice moisture based on hyperspectral imaging technology and BCC-LS-SVR algorithm. *J. Food Process Eng.* 40 (3), e12446. Article e12446. doi:10.1111/ffpe.12446
- Sun, J., Ge, X., Wu, X. H., Dai, C. X., and Yang, N. (2018). Identification of pesticide residues in lettuce leaves based on near infrared transmission spectroscopy. *J. Food Process Eng.* 41 (6), Article e12816. doi:10.1111/jfpe.12816
- Tang, P., Li, H., Issaka, Z., and Chen, C. (2017). Impact forces on the drive spoon of a large cannon irrigation sprinkler: simple theory, CFD numerical simulation and validation. *Biosyst. Eng.* 159, 1–9. doi:10.1016/j.biosystemseng.2017.04.005
- Tang, N. Q., Sun, J., Yao, K. S., Zhou, X., Tian, Y., Cao, Y., et al. (2021). Identification of Lycium barbarum varieties based on hyperspectral imaging technique and competitive adaptive reweighted sampling-whale optimization algorithm-support vector machine. *J. Food Process Eng.* 44 (1). doi:10.1111/jfpe.13603
- Tao, L., Feng, Z., Jiang, Y., Mo, N., and Liu, Y. (2024). A hardness-based constitutive model for numerical simulation of blind rivet with gradient hardness distribution. *Mater. Today Commun.* 39, 109331. doi:10.1016/j.mtcomm.2024.109331
- Tao, L., Feng, Z., Jiang, Y., Lu, R., and Mo, N. (2025). Strain gradient-driven microstructural evolution and strengthening mechanisms in post-riveting bulged region of A286 superalloy blind rivets. *J. Mater. Process. Technol.* 343, 118955. doi:10.1016/j.jmatprotec.2025.118955
- Tian, L., Jiangfeng, S., Ang, Z., Guoqiang, Y., Yan, Y., Bin, J., et al. (2023). Progress and prospects in Mg-alloy super-sized high pressure die casting for automotive structural components. *J. Magnesium Alloys* 11 (11), 4166–4180. doi:10.1016/j.jma.2023.11.003
- Vorderbrüggen, J., Köhler, D., Grüber, B., Troschitz, J., Gude, M., and Meschut, G. (2022). Development of a rivet geometry for solid self-piercing riveting of thermally loaded CFRP-metal joints in automotive construction. *Compos. Struct.* 291, 115583. doi:10.1016/j.compstruct.2022.115583
- Wang, J., and Chen, R. (2020). An improved finite element model for the hydraulic analysis of drip irrigation subunits considering local emitter head loss. *Irrigation Sci.* 38 (No.2), 147-162. doi:10.1007/s00271-019-00656-0
- Wang, C., Du, Z., Cheng, A., He, Z., Tan, H., and Yu, W. (2023). Influence of process parameters and heat treatment on self-piercing riveting of high-strength steel and die-casting aluminium. *J. Mater. Res. Technol.* 26, 8857–8878. doi:10.1016/j.jmrt.2023.09.187
- Wang, W., Wang, K., Khan, H. A., Li, J., and Miller, S. (2018). Numerical analysis of magnesium to aluminum joints in friction stir blind riveting. *Procedia CIRP* 76, 94–99. doi:10.1016/j.procir.2018.01.037
- Wang, C.-x., Suo, T., Gao, H.-m., and Xue, P. (2019). Determination of constitutive parameters for predicting dynamic behavior and failure of riveted joint: testing, modeling and validation. *Int. J. Impact Eng.* 132, 103319. doi:10.1016/j.ijimpeng.2019.103319
- Wang, W., Lv, X., and Yi, Z. (2022). Parameter optimization of reciprocating cutter for Chinese little greens based on finite element simulation and experiment. AGRICULTURE-BASEL 12 (No.12), 2131–18. doi:10.3390/agriculture12122131
- Wang, B. Z., Chen, S. R., Wang, G. Q., Tang, Z., and Ding, H. T. (2024a). Damping optimization method of combine harvester frame undergoing multi-source excitation. *Agriculture-Basel* 14 (6), 815. doi:10.3390/agriculture14060815
- Wang, C., Du, Z., Cheng, A., and He, Z. (2024b). Numerical investigation of joinability and forming quality improvement on self-piercing riveting process with varying sheet stack combinations. *Thin-Walled Struct.* 201, 112017. doi:10.1016/j.tws.2024.112017
- Wang, C., Yu, W., Cheng, A., and He, Z. (2024c). Study on the failure mechanism and mechanical properties of multi-layer hole-drilled self-piercing riveted three-layer steel/aluminum hybrid joints. *Eng. Fail. Anal.* 164, 108681. doi:10.1016/j.engfailanal.2024.108681
- Wang, G., Bao, Z., Gao, Z., Sun, W., Zhang, W., and Liu, Y. (2024d). Optimization of blind riveting process parameters of aluminum alloy based on finite element simulation. *Mater. Today Commun.* 41, 111078. doi:10.1016/j.mtcomm.2024.
- Wang, L., Liang, D., Yu, R., Wang, M., Tian, Y., Ma, T., et al. (2024e). Progress and prospects in magnesium alloy scrap recycling. *J. Magnesium Alloys* 12 (12), 4828–4867. doi:10.1016/j.jma.2024.11.031
- Wang, L., Wang, G., Zhai, X., Tang, Z., Wang, B., and Li, P. (2024f). Response characteristics of harvester bolts and the establishment of the strongest response structure's kinetic model. *Agriculture* 14 (7), 1174. doi:10.3390/agriculture14071174

- Wang, C., Cheng, A., Qin, Q., Zhang, F., Liao, Z., and He, Z. (2025a). Study on mechanical degradation and corrosion behavior of pre-holed self-piercing riveted-bonded hybrid joints under salt spray condition. *Eng. Fail. Anal.* 170, 109304. doi:10.1016/j.engfailanal.2025.109304
- Wang, C., Hu, Z., Cheng, A., and Du, Z. (2025b). Mechanical properties and failure mechanism of steel/aluminum pre-holed self-piercing riveted joints under different loading speeds and loading types: an experimental and numerical investigation. *Int. J. Impact Eng.* 206, 105453. doi:10.1016/j.ijimpeng.2025.105453
- Wang, C., Yu, W., Cheng, A., and He, Z. (2025c). Study on the effects of hole diameter and sheet thickness on quasi-static and fatigue behaviors of pre-holed self-piercing riveted steel-aluminium joints. *Int. J. Fatigue* 193, 108761. doi:10.1016/j.ijfatigue.2024.108761
- Wang, Y., Cao, Z., Zheng, G., Zhang, M., Wang, X., and Zuo, D. (2023). Analysis of TB2 rivet forming quality and mechanical properties of thin sheet riveted joints based on different riveting methods. *Eng. Fail. Anal.* 154, 107666. doi:10.1016/j.engfailanal.2023.107666
- Weiqi, P., Yue, Z., and Tianmu, X. (2023). A review of the feasibility of aluminum alloys, carbon fiber composites and glass fiber composites for vehicle weight reduction in the automotive industry. *J. Phys. Conf. Ser.* 2608 (1), 012005. doi:10.1088/1742-6596/2608/1/012005
- Wen, H., Jin, J., Yang, W., Liao, Y., Li, G., Cui, J., et al. (2024). Failure analysis of CFRP-aluminum electromagnetic self-pierce riveting-bonded joints subjected to highspeed loading. *Eng. Fail. Anal.* 164, 108691. doi:10.1016/j.engfailanal.2024.108691
- Wu, H., Wang, M., Liu, S., Han, Y., Zheng, Y., and Li, X. (2025). Enhancing joint performance with reshaping self-piercing riveting: a comparative study of die structures and optimization techniques. *Thin-Walled Struct.* 213, 113220. doi:10.1016/j.tws.2025.113220
- Xian, X., Ma, Y., Shan, H., Niu, S., and Li, Y. (2019). Single-sided joining of aluminum alloys using friction self-piercing riveting (F-SPR) process. *J. Manuf. Process.* 38, 319–327. doi:10.1016/j.jmapro.2019.01.037
- Xie, Z. X., Fan, X. G., Wang, L., Zhan, M., and Ma, F. (2026). Stepwise cooling spinning to achieve isotropic strength-ductility synergy of titanium alloy tube. *J. Mater. Sci. Technol.* 244, 156–172. doi:10.1016/j.jmst.2025.03.106
- Xu, W., and Wang, D. (2021). Material–structure–process–performance integration multi-objective optimization design for solid rivet joint. *J. Mater. Eng. Perform.* 30 (8), 5541–5556. doi:10.1007/s11665-021-05807-z
- Xu, L. Z., Hansen, A. C., Li, Y. M., Liang, Z. W., and Yu, L. J. (2016). Numerical and experimental analysis of airflow in a multi-duct cleaning system for a rice combine harvester. *Trans. Asabe* 59 (5), 1101–1110. doi:10.13031/trans.59.11569
- Xu, L., Li, Y., Chai, X., Wang, G., Liang, Z., Li, Y., et al. (2020). Numerical simulation of gas-solid two-phase flow to predict the cleaning performance of rice combine harvesters. *Biosyst. Eng.* 190, 11–24. doi:10.1016/j.biosystemseng.2019.11.014
- Yang, B., Ma, Y., Shan, H., Niu, S., and Li, Y. (2022a). Friction self-piercing riveting (F-SPR) of aluminum alloy to magnesium alloy using a flat die. *J. Magnesium Alloys* 10 (5), 1207–1219. doi:10.1016/j.jma.2020.12.016
- Yang, B., Shan, H., Liang, Y., Ma, Y., Niu, S., Zhu, X., et al. (2022b). Effect of adhesive application on friction self-piercing riveting (F-SPR) process of AA7075-T6 aluminum alloy. *J. Mater. Process. Technol.* 299, 117336. doi:10.1016/j.jmatprotec.2021.117336
- Yang, J., Zhu, Z., Han, S., Gu, Y., Zhu, Z., and Zhang, H. (2024). Evolution, limitations, advantages, and future challenges of magnesium alloys as materials for aerospace applications. *J. Alloys Compd.* 1008, 176707. doi:10.1016/j.jallcom.2024.176707
- Yang, L., Yang, G., Yu, D., Jiang, L., Chen, D., Yuan, Y., et al. (2025). Strength characteristics analysis and unified model establishment of bonded, riveted, and adhesive-rivet hybrid CFRP joints. *Eng. Struct.* 322, 119121. doi:10.1016/j.engstruct.2024.119121
- Yılmaz, T. G., Tüfekçi, M., and Karpat, F. (2017). A study of lightweight door hinges of commercial vehicles using aluminum instead of steel for sustainable transportation. Sustainability 9 (10), 1661. doi:10.3390/su9101661
- Ying, L., Gao, T., Dai, M., Hu, P., and Dai, J. (2021). Towards joinability of thermal self-piercing riveting for AA7075-T6 aluminum alloy sheets under quasi-static loading conditions. *Int. J. Mech. Sci.* 189, 105978. doi:10.1016/j.ijmecsci.2020.105978
- Ying, L., Dong, Q., Gao, T., Dai, M., and Hu, P. (2024). Self-piercing riveting of dissimilar carbon fiber-reinforced composites and aluminum alloy sheets: state-of-the-art achievements. *Int. J. Adv. Manuf. Technol.* 130 (1), 1–22. doi:10.1007/s00170-023-12506-3
- Yu, F., Tang, H., Zhang, B., Wan, H., Zhu, F., Zheng, W., et al. (2025). Achieving high strength and defect suppression in CFRP/aluminum alloy single-sided friction riveted joints *via* novel threaded rivets. *J. Mater. Process. Technol.* 345, 119054. doi:10.1016/j.jmatprotec.2025.119054
- Yuan, H., Cai, Y., Liang, S. F., Ku, J. S., and Qin, Y. (2023). Numerical simulation and analysis of feeding uniformity of viscous miscellaneous fish bait based on EDEM software. *Agriculture-Basel* 13 (2), 356. doi:10.3390/agriculture13020356
- Yuan, J., Ma, Y., Liu, Y., Xu, W., Ma, N., and Li, Y. (2025). Fatigue behavior and failure mechanism of friction self-piercing riveted aluminum alloy 2060-T8 joints. *Int. J. Fatigue* 197, 108940. doi:10.1016/j.ijfatigue.2025.108940

YunWu, M., Ming, L., YongBing, L., and ZhongQin, L. (2017). Effect of rivet and die on self-piercing rivetability of AA6061-T6 and mild steel CR4 of different gauges. *J. Mater. Process. Tech* 251, 282–294. doi:10.1016/j.jmatprotec.2017.08.020

- Zhan, L., Kong, C., Zhao, C., Cui, X., Zhang, L., Song, Y., et al. (2025). Recent advances on magnesium alloys for automotive cabin components: materials, applications, and challenges. *J. Mater. Res. Technol.* 36, 9924–9961. doi:10.1016/j.jmrt.2025.05.105
- Zhang, X., Zhang, M., Sun, L., and Li, C. (2018). Numerical simulation and experimental investigations on TA1 titanium alloy rivet in electromagnetic riveting. *Archives Civ. Mech. Eng.* 18 (3), 887–901. doi:10.1016/j.acme.2018.01.003
- Zhang, X., Jiang, H., Luo, T., Hu, L., Li, G., and Cui, J. (2019). Theoretical and experimental investigation on interference fit in electromagnetic riveting. *Int. J. Mech. Sci.* 156, 261–271. doi:10.1016/j.ijmecsci.2019.04.002
- Zhang, X., He, X., Xing, B., Wei, W., and Lu, J. (2020). Pre-holed self-piercing riveting of carbon fibre reinforced polymer laminates and commercially pure titanium sheets. *J. Mater. Process. Technol.* 279, 116550. doi:10.1016/j.jmatprotec.2019.116550
- Zhang, K., Min, J., Wan, H., Liao, P., and Lin, J. (2022). Thermo-mechanical modeling of flow drilling with a conical-tipped blind rivet. *CIRP J. Manuf. Sci. Technol.* 36, 158–171. doi:10.1016/j.cirpj.2021.12.003
- Zhang, P., Zhao, S.-d., Zhang, C.-w., Zang, S.-l., Chen, Z., Fei, L.-y., et al. (2022). Bonding mode and mechanical properties of keyhole-free friction stir rivet welded aluminum alloy joints. *J. Mater. Res. Technol.* 18, 185–199. doi:10.1016/j.jmrt.2022.02.097
- Zhang, H., Song, Z., Zhang, L., Liu, Z., and Zhu, P. (2023). Effects of hygrothermal ageing and temperature on the mechanical behavior of aluminum-CFRP hybrid (riveted/bonded) joints. *Int. J. Adhesion Adhesives* 121, 103299. doi:10.1016/j.ijadhadh.2022.103299
- Zhang, J., Miao, J., Balasubramani, N., Cho, D. H., Avey, T., Chang, C.-Y., et al. (2023). Magnesium research and applications: past, present and future. *J. Magnesium Alloys* 11 (11), 3867–3895. doi:10.1016/j.jma.2023.11.007
- Zhang, B., Ma, Y., Yu, F., Liu, Y., Zhou, E., Fan, Z., et al. (2024). Strengthening flat-die friction self-pierce riveting joints *via* manipulating stir zone geometry by tailored rivet structures. *Int. J. Mach. Tools Manuf.* 203, 104223. doi:10.1016/j.ijmachtools.2024.104223

- Zhang, Z., Zeng, K., Xing, B., and Shu, B. (2024). Finite element modeling and analysis of the self-piercing riveting forming process with the ball-shaped die. *Mater. Today Commun.* 39, 109267. doi:10.1016/j.mtcomm.2024.109267
- Zhang, X., Chen, N., Zhang, J., Tong, Y., Liu, P., Zhu, W., et al. (2025a). Effect of prefabricated cracks on microstructure evolution and mechanical properties of electromagnetic riveted joints. *Eng. Fail. Anal.* 169, 109190. doi:10.1016/j.engfailanal.2024.109190
- Zhang, X., Gao, Y., Zhang, Q., and Xie, Y. (2025b). Reshaping, performance optimization and failure mechanisms of self-piercing riveted joints in 5083 aluminum alloys under axial compressive loads. *Eng. Fail. Anal.* 176, 109631. doi:10.1016/j.engfailanal.2025.109631
- Zhao Z., Z., Li, H. C., Liu, J. K., and Yang, S. X. (2020). Control method of seedbed compactness based on fragment soil compaction dynamic characteristics. *SOIL TILLAGE Res.* 198 (No.0), 104551. doi:10.1016/j.still.2019.104551
- Zhao, J., Peng, Y., Su, W., and Dong, J. (2021). Finite element analysis of the shear capacity of stainless-steel blind-rivet connections. *J. Constr. Steel Res.* 179, 106558. doi:10.1016/j.jcsr.2021.106558
- Zhao, H., Han, L., Liu, Y., and Liu, X. (2022). Analysis of joint formation mechanisms for self-piercing riveting (SPR) process with varying joining parameters. *J. Manuf. Process*. 73, 668–685. doi:10.1016/j.jmapro.2021.11.038
- Zhao, Y., Wang, H., Li, H., He, J., Zhou, Y., Liu, J., et al. (2023). Competitive fretting fatigue failure analysis of Al alloy–CFRP riveted and adhesive–riveted single-shear lap joints. *Eng. Fail. Anal.* 153, 107538. doi:10.1016/j.engfailanal.2023.107538
- Zhou, X., Sun, J., Tian, Y., Wu, X. H., Dai, C. X., and Li, B. (2019). Spectral classification of lettuce cadmium stress based on information fusion and VISSA-GOA-SVM algorithm. *J. Food Process Eng.* 42 (5), Article e13085. doi:10.1111/jfpe.13085
- Zhou, X., Jun, S., Yan, T., Bing, L., Hang, Y. Y., and Quansheng, C. (2020). Hyperspectral technique combined with deep learning algorithm for detection of compound heavy metals in lettuce. *Food Chem.* 321, 126503. doi:10.1016/j.foodchem.2020.126503
- Zhu, Q. Z., Zhang, H. Y., Zhu, Z. H., Gao, Y. Y., and Chen, L. P. (2022). Structural design and simulation of pneumatic conveying line for a paddy side-deep fertilisation system. *Agriculture-Basel* 12 (6), 867. doi:10.3390/agriculture12060867